

**THE POTENTIAL OF CARBONYL SULFIDE AS A PROXY FOR GROSS
PRIMARY PRODUCTION AT FLUX TOWER SITES**

by

J. Mark Blonquist Jr.

A thesis submitted to the faculty of
The University of Utah
in partial fulfillment of the requirements for the degree of

Master of Science

Department of Biology

The University of Utah

August 2012

Copyright © J. Mark Blonquist Jr. 2012

All Rights Reserved

The University of Utah Graduate School

STATEMENT OF THESIS APPROVAL

The thesis of J. Mark Blonquist Jr.

has been approved by the following supervisory committee members:

<u>David R. Bowling</u>	, Chair	<u>June 15, 2012</u> <small>Date Approved</small>
-------------------------	---------	--

<u>John S. Sperry</u>	, Member	<u>June 15, 2012</u> <small>Date Approved</small>
-----------------------	----------	--

<u>Courtenay Strong</u>	, Member	<u>June 15, 2012</u> <small>Date Approved</small>
-------------------------	----------	--

and by Neil J. Vickers, Chair of
the Department of Biology

and by Charles A. Wight, Dean of The Graduate School.

ABSTRACT

Seasonal dynamics of atmospheric carbonyl sulfide (OCS) at regional and continental scales and plant OCS exchange at the leaf level have shown a close relationship with those for CO₂. CO₂ has both sinks and sources within terrestrial ecosystems, but the primary terrestrial exchange for OCS is thought to be leaf uptake, suggesting potential for OCS uptake as a proxy for gross primary production (GPP). The utility of OCS uptake as a GPP proxy in micrometeorological studies of biosphere-atmosphere CO₂ exchange was explored by applying theoretical concepts from earlier OCS studies to estimate GPP. Measured net ecosystem exchange (NEE) was partitioned using the ratio of measured vertical mole fraction gradients of OCS and CO₂. At the Harvard Forest AmeriFlux site, measured CO₂ and OCS vertical gradients were correlated, and were related to NEE and GPP, respectively. Estimates of GPP from OCS-based NEE partitioning were similar to those from established regression techniques, providing evidence that OCS uptake can potentially serve as a GPP proxy. Measured vertical CO₂ mole fraction gradients at five other AmeriFlux sites were used to project anticipated vertical OCS mole fraction gradients to provide indication of potential OCS signal magnitudes at sites where no OCS measurements were made. Projected OCS gradients at sites with short canopies were greater than those in forests, including measured OCS gradients at Harvard Forest, indicating greater potential for OCS uptake as a GPP proxy at these sites. This exploratory study suggests that continued investigation of linkages between OCS and GPP is warranted.

TABLE OF CONTENTS

ABSTRACT	iii
LIST OF TABLES	v
LIST OF FIGURES	vi
ACKNOWLEDGEMENTS	ix
INTRODUCTION	1
THEORY	4
MATERIALS AND METHODS	13
Flux Tower Observations: General	13
Harvard Forest: OCS Mole Fraction Measurements	15
Harvard Forest: CO ₂ Mole Fraction and CO ₂ Flux Measurements	16
Harvard Forest: CO ₂ and OCS Gradients and Ecosystem Relative Uptake (ERU)	17
Harvard Forest: Comparison of GPP Estimates and Uncertainties	20
Harvard Forest: Estimation of OCS Flux Magnitude and Above-canopy OCS Gradients	21
Projection of OCS Gradients at Additional AmeriFlux Sites	22
RESULTS	24
Harvard Forest	24
Anticipated OCS Gradients at the Additional Sites	31
DISCUSSION	34
Harvard Forest	34
Anticipated OCS Gradients at the Additional Sites	40
CONCLUSIONS	43
REFERENCES	45

LIST OF TABLES

Table	Page
1. Characteristics of AmeriFlux sites evaluated in this study	14
2. Summary of linear regression statistics for measured CO ₂ mole fraction gradients versus net ecosystem exchange (NEE) and projected OCS mole fraction gradients versus gross primary production (GPP _{TER}) at all sites evaluated (site details are provided in Table 1)	33
3. Summary of measured CO ₂ mole fraction gradients and projected OCS mole fraction gradients at all sites evaluated (site details are provided in Table 1).....	33

LIST OF FIGURES

Figure	Page
<p>1. Modeled values of leaf relative uptake (LRU). a Leaf relative uptake (leaf-level OCS flux normalized by OCS mole fraction, divided by leaf-level CO₂ flux normalized by CO₂ mole fraction) calculated from Eq. 6 and plotted versus intercellular to ambient CO₂ mole fraction ratio (C_{iCO_2} / C_{aCO_2}) for three different OCS stomatal to internal conductance ratios (g_{sOCS} / g_{iOCS}). b Same as in a, but for three different mesophyll to ambient OCS mole fraction ratios (C_{mOCS} / C_{aOCS}). The values of $g_{sOCS} / g_{iOCS} = 0.2$ and $C_{mOCS} / C_{aOCS} = 0.08$ were taken from Stimler et al. (2010a) and are assumed representative of C₃ vegetation; the other g_{sOCS} / g_{iOCS} (0.1, 0.5) and C_{mOCS} / C_{aOCS} (0.0, 0.2) values show how the relationship between LRU and C_{iCO_2} / C_{aCO_2} changes when g_{sOCS} / g_{iOCS} and C_{mOCS} / C_{aOCS} vary</p>	12
<p>2. Measured within-canopy gas profiles at Harvard Forest. Mean normalized a CO₂, b O₃, and c OCS mole fraction profiles calculated from the 12 days during the 2006 growing season when OCS measurements were made. Normalized mole fractions were calculated by dividing the mole fraction at each height by the mole fraction at 29.0 m; error bars show standard deviation of the mean at each height (in some cases error bars are smaller than symbols). Two OCS profiles are shown: linear profile between 29.0 and 2.0 m (the only two heights at which OCS mole fractions were measured) and an OCS profile with an estimated datum at 18.3 m (square symbol in c), which was based on the shape of the O₃ profiles measured at the time of air sample collection for OCS analysis and calculated from Eq. 7. OCS data were typically collected within 3 hours of local noon and within- and above-canopy measurements were typically made within less than 2 hours of each other; CO₂ and O₃ data are mean values calculated from half-hourly means corresponding to the time of OCS measurements</p>	18
<p>3. Seasonal patterns of photosynthesis, and carbon dioxide (CO₂) and carbonyl sulfide (OCS) mole fractions at Harvard Forest. a Harvard Forest gross primary production estimates from net ecosystem exchange partitioning via the method of Reichstein et al. (2005) (GPP_{TER}), b CO₂ mole fraction measurements at 29.0 m, and c OCS mole fraction measurements at 29.0 m. GPP_{TER} and CO₂ data are mean values calculated from 8 half-hourly means centered on local noon; OCS data are from air samples typically collected within 3 hours of local noon. Solid lines are 31 day means centered on each day of year</p>	25
<p>4. Carbon dioxide (CO₂) and carbonyl sulfide (OCS) gradients as a function of driving variables Harvard Forest. CO₂ gradients (CO₂ at 18.3 m minus CO₂ at 29.0 m, divided by the height difference) versus a net ecosystem exchange (NEE) ($y = 0.0053x + 0.015$, $r^2 = 0.16$, slope $P < 0.001$, intercept n.s.) and c friction velocity ($y = 0.11x - 0.12$, $r^2 = 0.04$, slope $P < 0.025$, intercept $P < 0.001$). Harvard Forest OCS gradients, assuming a linear OCS profile (OCS at 2.0 m minus OCS at 29.0 m, divided by the height difference), versus b gross primary production</p>	

estimates from NEE partitioning via the method of Reichstein et al. (2005) (GPP_{TER}) ($y = 0.015x - 0.085$, $r^2 = 0.17$, slope $P < 0.05$, intercept n.s.) and **d** friction velocity ($y = 0.66x - 0.70$, $r^2 = 0.09$, slope n.s., intercept $P < 0.05$). OCS data were typically collected within 3 hours of local noon and within-canopy and above-canopy measurements were typically made within less than 2 hours of each other; CO_2 , NEE, GPP_{TER} , and friction velocity data points are mean values calculated from half-hourly means corresponding to the time of OCS measurements 26

5. Relative OCS gradients (calculated from Eq. 2) versus relative CO_2 gradients (calculated from Eq. 3) at Harvard Forest. CO_2 gradients were directly calculated from mole fraction measurements at 29.0 m and 18.3 m. OCS gradients were calculated for the 29.0 m and 18.3 m height difference using mole fraction measurements at 29.0 m and 2.0 m and **a** assuming a linear profile between 29.0 m and 2.0 m ($y = 4.26x - 0.00$, $r^2 = 0.61$, slope $P < 0.01$, intercept n.s.), and **b** estimating the OCS mole fraction at 18.3 m based on the shape of the O_3 profiles measured at the time of air sample collection for OCS analysis (Eq. 7) ($y = 3.28x + 0.00$; $r^2 = 0.76$; slope $P < 0.001$, intercept n.s.). Data are from the 2006 growing season only, and slopes of the lines are representative of ERU over the time period when the data were collected, day of year 160 to 296. OCS data were typically collected within 3 hours of local noon and within- and above-canopy measurements were typically made within less than 2 hours of each other; CO_2 data are mean values calculated from half-hourly means corresponding to the time period of OCS measurements 27
6. Harvard Forest gross primary production estimates from net ecosystem exchange partitioning via the method of Reichstein et al. (2005) (GPP_{TER}) and Eq. 5 (GPP_{OCS}). In **a** and **b** GPP_{OCS} was calculated for 9 different days based on the short-term ERU estimate for each day; ERU was estimated from the **a** linear OCS profile ($y = 1.26x - 4.31$, $r^2 = 0.37$, $P < 0.1$), and **b** O_3 -shaped OCS profile ($y = 0.82x + 2.30$, $r^2 = 0.44$, $P < 0.05$). In **c** and **d** GPP_{OCS} was derived from NEE scaled by the growing season ERU values taken from the slopes of the lines in Fig. 5 (ERU from linear OCS profiles = 4.3 and ERU from O_3 -shaped OCS profiles = 3.3). OCS measurements spanned day of year 160 to 296 in 2006; **b** mean midday GPP for all days ($y = 1.28x + 3.11$, $r^2 = 0.99$, slope $P < 0.001$, s.e. of slope = 0.01 for ERU = 4.3 and $y = 0.99x + 2.39$, $r^2 = 0.99$, slope $P < 0.001$, s.e. of slope = 0.01 for ERU = 3.3) and **d** sum of GPP during daylight hours for all days. In all panels leaf relative uptake (LRU in Eq. 5) was estimated as 3 (calculated from Eq. 6). OCS data were typically collected within 3 hours of local noon and within- and above-canopy measurements were typically made within less than 2 hours of each other; GPP_{TER} data are mean values calculated from half-hourly means corresponding to the time period of OCS measurements 29
7. Estimates of above-canopy carbonyl sulfide (OCS) fluxes and gradients at Harvard Forest. **a** OCS fluxes estimated from gross primary production estimates from net ecosystem exchange partitioning via the method of Reichstein et al. (2005) (GPP_{TER}) and **b** above-canopy (surface layer) OCS gradients estimated from Monin-Obukhov Similarity Theory (MOST) for 2006. OCS flux estimates were calculated from Eq. 1 using only above-canopy CO_2 and OCS mole fraction measurements and GPP_{TER} . Leaf relative uptake (LRU in Eq. 1) was estimated as 3 (calculated from Eq. 6). OCS gradient estimates were calculated from Eq. 8 using the OCS flux estimates from **a** and friction velocity measurements at 29.0 m (flux measurement height). GPP_{TER} and CO_2 data used to estimate OCS fluxes and friction velocity data used to estimate OCS gradients were mean values calculated from 8 half-hourly means

centered on local noon; OCS data used in the estimate were from air samples typically collected within 3 hours of local noon. The solid line is a 31 day mean centered on each day of year. Only data from 2006 are shown because simultaneous above-canopy CO₂ and OCS measurements were unavailable due to missing CO₂ data on many of the days in 2005 30

8. Relationship between measured CO₂ gradients (within- minus above-canopy CO₂ mole fraction, divided by the difference between measurement heights) and measured net ecosystem exchange (NEE) (left panels), and projected OCS gradients and gross primary production estimates from NEE partitioning via the method of Reichstein et al. (2005) (GPP_{TER}) (right panels), at all six AmeriFlux sites evaluated. Projected OCS gradients were calculated with Eqs. 2-4, assuming co-located measurement heights for OCS and CO₂, an ecosystem relative uptake (ERU) of 4, and an above-canopy OCS mole fraction of 400 pmol mol⁻¹ (assumptions produce projected OCS gradients for the same time frame and height difference as CO₂ gradients). All data are mean values calculated from 8 half-hourly means centered on local noon. Ameriflux site details are given in Table 1, statistics for the linear regressions are given in Table 2, and summary statistics for CO₂ and OCS gradients at each site are given in Table 3 32

ACKNOWLEDGEMENTS

I extend special thanks to my committee members, David Bowling, John Sperry, and Court Strong, for their encouragement and support. In particular, I extend special thanks to David Bowling for his guidance and patience while working with me on this project and others during my time in his laboratory. In addition to the excellent scientific mentoring he provided, he has been extremely supportive of my ideas and respectful of my decisions. I consider him a trainer and friend.

I extend sincere thanks to Steve Montzka, Bill Munger, Dan Yakir, Ankur Desai, Danilo Dragoni, Tim Griffis, Russ Monson, and Russ Scott for providing data from AmeriFlux sites, reviewing drafts of the thesis, providing insightful and encouraging suggestions, and helping me address comments and concerns from the peer review process. I also extend thanks to Elaine Gottlieb for her role in collecting the within-canopy OCS samples at Harvard Forest; John Baker, Sean Burns, Ken Davis, and Hans-Peter Schmid for sharing AmeriFlux data; John Miller for thoughtful ideas and discussion; Tom Boden and the CDIAC staff for maintaining the AmeriFlux data archive; Markus Reichstein for maintaining the flux data gap-filling and flux-partitioning website; and Ryan Campbell for reviewing an early version of the thesis.

I gratefully acknowledge support from the National Science Foundation Division of Graduate Education, grant DGE08-41233; the University of Utah; and the Office of Science (BER), US Department of Energy, Grant DE-SC0005236. Any opinions, findings, and conclusions or recommendations expressed in this thesis are those of the author and do not necessarily reflect the views of the DOE.

OCS measurements were supported in part by the Atmospheric Composition and Climate Program of the National Oceanic and Atmospheric Administration's Climate Program Office. Observations at Harvard Forest were supported by the Office of Science (BER), U.S. Department of Energy, grant DE-FG02-07ER64358, and through the Northeastern Regional Center of the National Institute for Climate Change Research (3452-HU-DOE-4157). Observations at Morgan Monroe State Forest were supported by the Office of Science (BER), U.S. Department of Energy, through the Midwestern Center of the National Institute for Global Environmental Change (NIGEC), grant DE-FC03-90ER61010, and from BER, grant DE-FG02-07ER64371. Observations at Willow Creek were supported by the Office of Science (BER), U.S. Department of Energy, through the Midwestern Regional Center of the National Institute for Global Environmental Change, under Cooperative Agreement No. DE-FC03-90ER61010, and USDA Northern Research Station Joint Venture, agreement 09-JV-11242306-105, and the Wisconsin Focus on Energy. Observations at Niwot Ridge were supported by the Western Section of the National Institute for Climate Change Research (NICCR), which was supported by the Office of Biological Research at the Department of Energy, and the Long-Term Research in Environmental Biology (LTREB) Program at the National Science Foundation. Observations at Kendall Grassland were supported by USDA-ARS. Observations at Rosemount were supported by the National Science Foundation, grant ATM-0546476, and the Office of Science (BER), U.S. Department of Energy, grant DE-FG02-06ER64316.

INTRODUCTION¹

The difference between gross primary production (GPP) and total ecosystem respiration (TER) equals net ecosystem exchange of CO₂ (NEE), a commonly measured flux at eddy covariance tower sites across the globe (Baldocchi et al. 2003). Investigation of GPP and TER provides important process-based information about biosphere-atmosphere carbon exchange. Unfortunately, GPP and TER cannot be measured directly during the daytime by eddy covariance and must be estimated using additional information from measurements and models. There are several methods available to estimate GPP and TER from NEE, including regression of nocturnal NEE with environmental driving variables (usually temperature) and extrapolation to daytime (Goulden et al. 1996; Reichstein et al. 2005); prediction of TER from light response models (Lasslop et al. 2010; Yi et al. 2004); scaling-up measurements made in leaf, stem, and soil chambers (Lavigne et al. 1997; Law et al. 1999; Zha et al. 2007); calculation from ecosystem process models (Baldocchi and Wilson 2001; Ogeé et al. 2003a; Sacks et al. 2007); and stable isotope approaches (Ogeé et al. 2003b; Zobitz et al. 2008). New methods are also emerging; for example, correlation analysis based on flux-variance similarity (Scanlon and Kustas 2010). The most common NEE partitioning approach is to estimate TER using a regression of NEE on turbulent nights (assumed equal to TER) against temperature, then extrapolation of the TER-

¹ The material for this thesis is reproduced by permission of American Geophysical Union and was previously published as: Blonquist Jr. JM, Montzka SA, Munger JW, Yakir D, Desai AR, Dragoni D, Griffis TJ, Monson RK, Scott RL, Bowling DR (2011) The potential of carbonyl sulfide as a proxy for gross primary production at flux tower sites. *J Geophys Res* 116:G04019 doi:10.1029/2011JG001723

temperature relationship to daytime periods, where GPP is then calculated as NEE minus TER (Reichstein et al. 2005).

Challenges and often large uncertainties are associated with each NEE partitioning method. For example, low nighttime turbulence and advection fluxes can result in problematic NEE measurements and make regression-based estimates uncertain (van Gorsel et al. 2009), light response models do not capture within-day variability (Reichstein et al. 2005), chamber measurements require scaling to represent the entire ecosystem (Lavigne et al. 1997), and stable isotope approaches are dependent on isotopic disequilibrium between GPP and TER, which is sometimes difficult to resolve (Ogee et al. 2004). Additionally, different NEE partitioning methods provide different estimates of GPP and TER, leading to fundamental uncertainty about the process of interest (Desai et al. 2008; Griffis et al. 2004; Lasslop et al. 2010; Stoy et al. 2006). Independent, measurement-based approaches to estimate GPP and TER are required.

Recent studies have suggested the utility of carbonyl sulfide (OCS) uptake as a proxy for GPP, based on the close relationship between seasonal dynamics of OCS and CO₂ mole fractions at regional and continental scales (Blake et al. 2008; Campbell et al. 2008; Montzka and Tans 2004; Montzka et al. 2007; Sandoval-Soto et al. 2005) and the link between OCS and CO₂ uptake at the leaf level (Seibt et al. 2010; Stimler et al. 2010a). OCS is the most abundant reduced sulfur gas in the atmosphere, with mole fractions ranging from approximately 300-550 pmol mol⁻¹ (pptv) near the surface, depending on season, and a global mean of approximately 500 pmol mol⁻¹ (Montzka et al. 2007). The tropospheric lifetime of OCS is relatively long, 2-4 years (Montzka et al. 2007; Suntharalingam et al. 2008), and the major OCS sinks are vegetation, soils, reaction with oxidizing radicals in the troposphere and stratosphere, and photolysis in the stratosphere; the major sources are oceans, volcanic eruptions, and anthropogenic emissions (e.g., biomass burning, coal-fired power plants, and certain industrial processes) (Watts 2000).

Seasonal variation in the northern hemisphere is largely influenced by terrestrial vegetation uptake, while variation in the southern hemisphere is largely influenced by oceanic fluxes (Kettle et al. 2002; Montzka et al. 2007). Studies of OCS aimed at understanding exchange in terrestrial ecosystems have measured OCS exchange in soils (Castro and Galloway 1991; Kesselmeier et al. 1999; Liu et al. 2010; Simmons et al. 1999; Steinbacher et al. 2004; Van Diest and Kesselmeier 2008) and vegetation (Brown and Bell 1986; Goldan et al. 1988; Kesselmeier and Merk 1993; Kluczewski et al. 1985; Sandoval-Soto et al. 2005; Yonemura et al. 2005).

The few flux tower-scale OCS studies that have been conducted suggest linkage to GPP (Bartell et al. 1993; Mihalopoulos et al. 1989; Mihalopoulos and Nguyen 2001; White et al. 2010; Xu et al. 2002), and thereby potential for OCS uptake as a proxy for GPP. The goal of this work is to explore the utility of OCS measurements as a means of quantitatively estimating GPP in micrometeorological studies. The following theory section contains a summary of relevant studies, including those conducted at the flux tower-scale. The theoretical framework necessary to estimate GPP from OCS measurements is also developed. Then, measured vertical OCS mole fraction gradients from a temperate deciduous forest (Harvard Forest AmeriFlux site) are presented and used to estimate GPP by partitioning measured NEE (from eddy covariance). These GPP estimates are compared to GPP estimates from a widely used NEE partitioning method (Reichstein et al. 2005). Finally, the potential of OCS measurements for estimating GPP at other AmeriFlux sites (where OCS was not measured) is evaluated by deriving vertical OCS mole fraction gradients from CO₂ mole fraction profile measurements, and analyzing the relationship to GPP.

THEORY

While the OCS studies that have been conducted suggest the possibility of OCS uptake as a GPP proxy, no studies have yet estimated GPP from OCS measurements. The following requirements (R1-R4) should be met for OCS uptake to be used as a GPP proxy at the flux tower-scale (land surface area of 10^2 - 10^6 m²):

- R1. OCS and CO₂ must diffuse along the same physical pathway from the atmosphere through stomata to the point in leaves where the first biochemical step of metabolism of the gases takes place (Stimler et al. 2010a).
- R2. OCS exchange must be a one-way flux from the atmosphere to leaves (no OCS compensation point or OCS release analogous to respiratory release of CO₂) (Stimler et al. 2010a).
- R3. OCS and CO₂ cannot directly or indirectly interact (no inhibitory/toxicity effects between the gases) (Stimler et al. 2010a).
- R4. Any other OCS fluxes within the ecosystem must be negligible compared to plant uptake (Campbell et al. 2008; Montzka et al. 2007).

In vitro studies of plant enzyme uptake of OCS have provided support for R2. Protoschill-Krebs and Kesselmeier (1992) showed that carbonic anhydrase (CA), PEP-C, and Rubisco can metabolize OCS, with the key enzyme being CA, which irreversibly hydrates OCS to form CO₂ and hydrogen sulfide (H₂S) (Notni et al. 2007). Protoschill-Krebs et al. (1996) found the affinity of CA for OCS was approximately 1,000 times greater than that for CO₂, with a strong linear relationship between CA and OCS consumption.

Leaf-level gas exchange studies have provided support for R1-R3. Stimler et al. (2010a) studied three C_3 species and found stomatal conductance to OCS in the dark was significantly reduced relative to in the light, and stomatal conductance to and assimilation of OCS were significantly reduced following fumigation with abscisic acid, demonstrating stomatal control of OCS exchange. Stimler et al. (2010a) also reported that emissions of OCS were not detectable when leaves were exposed to OCS-free air in the light, indicating there was no OCS release, nor compensation point. Additionally, they found that OCS uptake remained constant at elevated levels of CO_2 , and similarly, CO_2 uptake remained constant at elevated levels of OCS, indicating there were no apparent cross-interactions or inhibitory/toxicity effects between CO_2 and OCS within the mole fraction ranges tested. However, competitive inhibition of CA by CO_2 was found during OCS and CO_2 gas exchange measurements in decaying leaf litter (Kesselmeier and Hubert 2002), indicating this possibility in live plant leaves exists. Results from Stimler et al. (2010a) were consistent with leaf-level results from Sandoval-Soto et al. (2005), who studied four other C_3 species, and found that (1) OCS uptake was highly correlated to CO_2 uptake and stomatal conductance to CO_2 , (2) OCS uptake closely followed the light/dark cycle, and (3) CO_2 and OCS uptake rapidly declined to near zero following application of abscisic acid, all indicating OCS uptake occurred predominantly through stomata. Sandoval-Soto et al. (2005) also found OCS emission did not occur, even at low ambient OCS, indicating a minimal-to-negligible OCS compensation point.

The few OCS studies at the flux tower-scale have provided support for R1-R3. Bartell et al. (1993) estimated OCS flux from a wet meadow and found it followed a diel pattern (with maximum uptake near midday and near-zero exchange at night) and was related to CO_2 flux, water vapor flux, and photosynthetically active radiation (PAR), indicating stomatal control of OCS uptake. Results from Xu et al. (2002), who measured OCS flux over a spruce forest (with

relaxed eddy accumulation), were consistent and showed that during the day the forest was an OCS sink; OCS flux was also related to PAR, CO₂ flux, and water vapor flux.

Soil is a major component of terrestrial ecosystems and may influence OCS exchange at the flux tower-scale, while OCS fluxes from oceans, volcanic eruptions, reaction with oxidizing radicals, and anthropogenic emissions are likely to be minor (data from White et al. (2010) indicate the possibility of oceanic effects). Soil microbes contain CA (Wingate et al. 2009) and may assimilate and act as a sink for OCS. Additionally, soil OCS uptake has been shown to be dependent on soil physical properties (Van Diest and Kesselmeier 2008). Most studies have shown soils are OCS sinks when ambient air is injected into the flux chamber rather than OCS-free air (Castro and Galloway 1991; Geng and Mu 2004; Kesselmeier et al. 1999; Kuhn et al. 1999; Mihalopoulos and Nguyen 2001; Simmons et al. 1999; Steinbacher et al. 2004; Van Diest and Kesselmeier 2008; White et al. 2010), with the exception of paddy soils (Liu et al. 2010). However, soil OCS uptake appears to be small relative to vegetation uptake, providing support for R4. Vertical profile measurements of OCS over various ecosystems have shown significant near-surface drawdown, compared to above-canopy heights, indicating a surface OCS sink (Bartell et al. 1993; Mihalopoulos et al. 1989; Mihalopoulos and Nguyen 2001; White et al. 2010), with minor soil uptake compared to vegetation and/or ecosystem uptake (Mihalopoulos and Nguyen 2001; White et al. 2010). Steinbacher et al. (2004) measured soil uptake in a spruce forest, using surface chambers, and found OCS uptake was less than 1 % of total ecosystem OCS flux (total ecosystem flux was measured above the canopy by Xu et al. (2002)), indicating uptake was dominated by vegetation. Results from White et al. (2010) for a loblolly pine forest were consistent with those of Steinbacher et al. (2004), as soil OCS uptake measured with surface chambers was less than 5 % of estimated daytime uptake by vegetation (inferred from branch enclosures).

There are some flux tower scale studies that suggest complications to using OCS as a proxy for GPP. Daytime measurements of above-canopy OCS flux made by Xu et al. (2002) showed uptake by a spruce forest, but nocturnal emission (when GPP was zero). Thus, it is possible that OCS uptake measured during the day was a net flux representing the balance between OCS uptake and emission, violating R4. Vertical profile measurements of OCS have also indicated emission from a loblolly pine forest (Berresheim and Vulcan 1992). Emission of organic sulfur compounds from a forest canopy has been reported (Puxbaum and König 1997), but emission of OCS from a loblolly pine forest is puzzling in light of recent results from White et al. (2010), who found loblolly pine trees were an OCS sink, even at night when trees were not photosynthesizing. This phenomenon was thought to be due to non-zero nocturnal stomatal conductance in loblolly pines (Caird et al. 2007), resulting in nocturnal OCS uptake because CA activity is light-independent (Protoschill-Krebs et al. 1996). This does not necessarily impact the use of OCS measurements as a GPP proxy, as GPP is zero at night. More work is required to determine the ecosystems in which OCS exchange is dominated by vegetation and the extent to which other fluxes are non-negligible.

When requirements R1-R4 are satisfied, OCS measurements can be used to directly estimate GPP at the flux tower scale via one of two methods: (1) OCS flux measurements or (2) simultaneous OCS and CO₂ vertical gradient measurements. The first method is fully independent of NEE measurements, but requires (a) direct measurement of OCS fluxes (ideally by eddy covariance), (b) ambient CO₂ and OCS mole fraction measurements, and (c) incorporation of the leaf-level uptake relationship between OCS and CO₂, defined as leaf relative uptake (LRU) (Sandoval-Soto et al. 2005):

$$\text{GPP} = F_{\text{OCS}} \left(\frac{C_{\text{aCO}_2}}{C_{\text{aOCS}}} \right) \left(\frac{1}{\text{LRU}} \right) \quad (1)$$

where F_{OCS} is OCS flux [$\text{pmol m}^{-2} \text{s}^{-1}$], C_{aCO_2} is ambient CO_2 mole fraction [$\mu\text{mol mol}^{-1}$], and C_{aOCS} is ambient OCS mole fraction [pmol mol^{-1}]. LRU is calculated by dividing the normalized leaf-level OCS flux [$\text{mol m}^{-2} \text{s}^{-1}$] by the normalized leaf-level CO_2 flux [$\text{mol m}^{-2} \text{s}^{-1}$], where normalized fluxes are measured fluxes divided by OCS and CO_2 mole fractions, respectively. Sandoval-Soto et al. (2005) used Eq. 1 to estimate the global OCS sink from GPP estimates. Campbell et al. (2008) used Eq. 1 and an atmospheric transport model to simulate vertical atmospheric OCS profiles over land in the northern hemisphere and found measured and modeled OCS profiles agreed, indicating OCS drawdown in the troposphere was likely driven primarily by GPP.

The second method to estimate GPP does not require direct OCS flux measurements, but requires (a) NEE measurements, (b) OCS and CO_2 vertical gradient measurements, and (c) LRU. This method will only work when gradients can be analytically measured. The ratio of GPP to NEE is proportional to the relative gradient of OCS (RG_{OCS}) [m^{-1}] divided by the relative gradient of CO_2 (RG_{CO_2}) [m^{-1}], defined as ecosystem relative uptake (ERU) (Campbell et al. 2008):

$$\text{RG}_{\text{OCS}} = \frac{G_{\text{OCS}}}{C_{\text{aOCS}}} \quad (2)$$

$$\text{RG}_{\text{CO}_2} = \frac{G_{\text{CO}_2}}{C_{\text{aCO}_2}} \quad (3)$$

$$\text{ERU} = \frac{\text{RG}_{\text{OCS}}}{\text{RG}_{\text{CO}_2}} \quad (4)$$

$$\frac{\text{GPP}}{\text{NEE}} = \text{ERU} \left(\frac{1}{\text{LRU}} \right) \quad (5)$$

where RG_{OCS} [m^{-1}] and RG_{CO_2} [m^{-1}] at the flux tower-scale are near- or within-canopy OCS and CO_2 mole fraction gradients, G_{OCS} [$\text{pmol mol}^{-1} \text{m}^{-1}$] and G_{CO_2} [$\mu\text{mol mol}^{-1} \text{m}^{-1}$], respectively, normalized by C_{aOCS} and C_{aCO_2} . Rearrangement of Eq. 5 shows that the ratio of the relative vertical mole fraction gradients, ERU, is proportional to GPP / NEE scaled by the ratio of relative leaf exchange rates, LRU. We stress that gradients are not used to determine fluxes here, only to scale NEE to GPP. Thus, the ratio of relative uptakes, ERU / LRU, is used to scale a measured flux, NEE (from eddy covariance), to a related flux, GPP. Hence, problems associated with within-canopy gradient measurements and counter-gradient fluxes (Cellier and Brunet 1992; Denmead and Bradley 1985; Raupach 1979) are not critical limitations in this application. Aircraft measurements over the mid-western U.S. over multiple years have revealed a mean ERU for North America of between 5 and 6 during June-August, suggesting that on a relative basis net OCS uptake during summer is 5 to 6 times greater than net CO_2 uptake (Campbell et al. 2008; Montzka et al. 2007). This feature results from uptake of both gases primarily by vegetation, with the influence of two offsetting processes affecting CO_2 but not OCS: back diffusion of CO_2 out of leaves after it has been reversibly hydrated by CA (Notni et al. 2007; Stimler et al. 2010a), characterized by LRU, and release of CO_2 via cellular respiration, characterized by GPP / NEE.

Estimation of GPP via either method requires that LRU be measured or estimated. Leaf-level fluxes and mole fractions can be directly measured, but leaf CO_2 and OCS exchange measurements are time and labor intensive and are rarely made in the field. An alternative to direct measurement was proposed by Seibt et al. (2010):

$$\text{LRU} = \frac{\left(1 - \frac{C_{\text{mOCS}}}{C_{\text{aOCS}}}\right)}{R_{\text{CO}_2\text{-OCS}} \left(1 + \frac{g_{\text{sOCS}}}{g_{\text{iOCS}}}\right) \left(1 - \frac{C_{\text{iCO}_2}}{C_{\text{aCO}_2}}\right)} \quad (6)$$

where C_{mOCS} is mole fraction of OCS in mesophyll cells [pmol mol^{-1}], C_{iCO_2} is mole fraction of CO_2 in leaf intercellular air spaces [$\mu\text{mol mol}^{-1}$], $R_{\text{CO}_2\text{-OCS}}$ is the ratio of binary diffusivities (in air) of CO_2 and OCS (approximately 1.2 (Seibt et al. 2010)), g_{sOCS} is stomatal conductance to OCS [$\text{mol m}^{-2} \text{s}^{-1}$], and g_{iOCS} is internal conductance to OCS [$\text{mol m}^{-2} \text{s}^{-1}$] (conductance from leaf intercellular air spaces to mesophyll cells). Seibt et al. (2010) derived Eq. 6 on the basis of a shared diffusion pathway for OCS and CO_2 and a model for leaf OCS uptake analogous to gradient-based models for leaf water loss and CO_2 uptake. Conceptually separate diffusion endpoints for CO_2 and OCS were assumed in the derivation; CO_2 diffusion in air was terminated at leaf intercellular air spaces, but continues in liquid to the site of Rubisco; OCS diffusion was terminated inside mesophyll cells, at the hypothesized site of CA. As Seibt et al. (2010) indicated, the spatial distribution of CA is not known. However, they hypothesized a location upstream of Rubisco, inside mesophyll cells and directly adjacent to intercellular spaces, and considered this to be the actual endpoint for OCS. From this hypothesis, Seibt et al. (2010) simplified Eq. 6 by assuming that g_{iOCS} is much larger than g_{sOCS} and that C_{mOCS} was zero, based on observations that OCS emission does not occur (Sandoval-Soto et al. 2005; Stimler et al. 2010a).

Estimates of $g_{\text{sOCS}} / g_{\text{iOCS}}$ and $C_{\text{mOCS}} / C_{\text{aOCS}}$ are required to estimate LRU from Eq. 6. Based on OCS and CO_2 exchange measurements in C_3 leaves, Stimler et al. (2010a) provided estimates of gas mole fractions and conductances at each point along the OCS and CO_2 diffusion pathway from ambient air to leaf chloroplasts. They assumed the chloroplast surface inside mesophyll cells was the endpoint for OCS, and found that the OCS mole fraction at the chloroplast surface was near 40 pmol mol^{-1} , yielding $C_{\text{mOCS}} / C_{\text{aOCS}}$ of approximately 0.08 (ambient OCS mole fraction

was near $500 \text{ pmol mol}^{-1}$), rather than zero as assumed by Seibt et al. (2010). Stimler et al. (2010a) also found $g_{\text{sOCS}} / g_{\text{iOCS}}$ was approximately 0.2. When values of $C_{\text{mOCS}} / C_{\text{aOCS}} = 0.08$ and $g_{\text{sOCS}} / g_{\text{iOCS}} = 0.2$ were entered in Eq. 6, LRU ranged from 1.3 to 3.2 for a $C_{\text{iCO}_2} / C_{\text{aCO}_2}$ range of 0.5 to 0.8 (Fig. 1; see also Fig. 3 in Seibt et al. (2010)), which approximately spans C_3 ecosystems (Seibt et al. 2010). Other values of $C_{\text{mOCS}} / C_{\text{aOCS}}$ (0.0, 0.2) and $g_{\text{sOCS}} / g_{\text{iOCS}}$ (0.1, 0.5) provide indication of the sensitivity of LRU to these variables and show a similar range, and non-linear response, of LRU across a wide $C_{\text{iCO}_2} / C_{\text{aCO}_2}$ range (Fig. 1). It is assumed that biochemical demand for OCS is always high relative to supply, due to the high affinity of CA for OCS (Protoschill-Krebs et al. 1996). When $C_{\text{iCO}_2} / C_{\text{aCO}_2}$ is low, biochemical demand for CO_2 is high relative to supply. In this case, stomatal conductance largely controls fluxes, and relative fluxes are near 1.0 as a result, because $C_{\text{mOCS}} / C_{\text{aOCS}}$ and $C_{\text{iCO}_2} / C_{\text{aCO}_2}$ are similar in magnitude and stomatal conductances to OCS and CO_2 are similar in magnitude ($R_{\text{CO}_2\text{-OCS}} = 1.2$; from Seibt et al. (2010)). When $C_{\text{iCO}_2} / C_{\text{aCO}_2}$ is high, biochemical demand for CO_2 is low relative to supply. As a result, biochemical demand largely controls fluxes and relative fluxes are greater than 1.0, because $C_{\text{mOCS}} / C_{\text{aOCS}}$ is much lower than $C_{\text{iCO}_2} / C_{\text{aCO}_2}$, but stomatal conductances to OCS and CO_2 remain similar in magnitude. The LRU range estimated from Eq. 6 (Fig. 1) is close to the 1.4 to 3.4 range measured by Sandoval-Soto et al. (2005) for multiple species. Seibt et al. (2010) reported published values of LRU to range from 1.5 to 4.0, and derived a global mean LRU estimate of 2.8 ± 0.3 . Stimler et al. (2010a) found LRU to be variable, dependent on environmental conditions, but found the range for three C_3 species to be approximately 1.0-4.0, similar that reported by Seibt et al. (2010). The relationship between LRU and $C_{\text{iCO}_2} / C_{\text{aCO}_2}$ in Eq. 6 provides means to estimate LRU in Eqs. 1 and 5, but a limitation of these equations may be the LRU term, which would benefit from better characterization in future work.

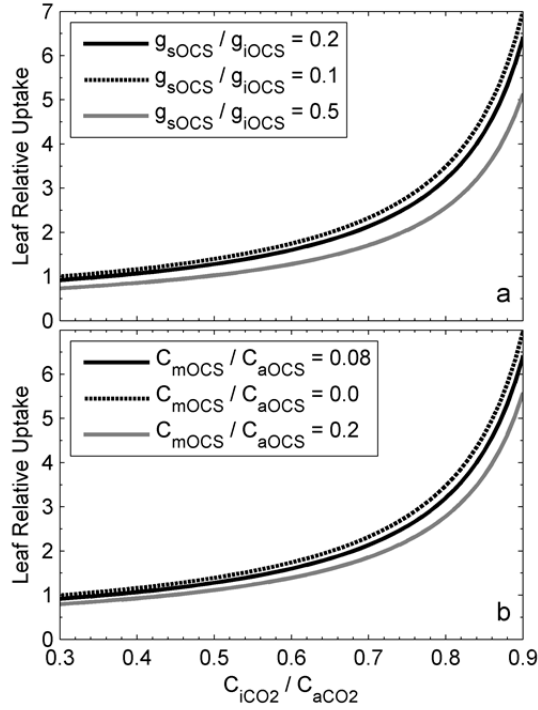


Fig. 1 Modeled values of leaf relative uptake (LRU). **a** Leaf relative uptake (leaf-level OCS flux normalized by OCS mole fraction, divided by leaf-level CO_2 flux normalized by CO_2 mole fraction) calculated from Eq. 6 and plotted versus intercellular to ambient CO_2 mole fraction ratio (C_{iCO_2} / C_{aCO_2}) for three different OCS stomatal to internal conductance ratios (g_{sOCS} / g_{iOCS}). **b** Same as in **a**, but for three different mesophyll to ambient OCS mole fraction ratios (C_{mOCS} / C_{aOCS}). The values of $g_{sOCS} / g_{iOCS} = 0.2$ and $C_{mOCS} / C_{aOCS} = 0.08$ were taken from Stimler et al. (2010a) and are assumed representative of C_3 vegetation; the other g_{sOCS} / g_{iOCS} (0.1, 0.5) and C_{mOCS} / C_{aOCS} (0.0, 0.2) values show how the relationship between LRU and C_{iCO_2} / C_{aCO_2} changes when g_{sOCS} / g_{iOCS} and C_{mOCS} / C_{aOCS} vary.

MATERIALS AND METHODS

A study at the Harvard Forest AmeriFlux site (Table 1) was conducted to explore the utility of OCS measurements to estimate GPP. Following analysis at Harvard Forest, the potential magnitude of OCS signals were evaluated at five other AmeriFlux sites (Table 1) using OCS projections from CO₂ measurements, as OCS measurements were only available at Harvard Forest.

Flux Tower Observations: General

For all sites, NEE, GPP, and friction velocity data were obtained from the Level 4 data archived on the AmeriFlux website (<http://public.ornl.gov/ameriflux/>). Level 4 flux data provide measured (with standard eddy covariance techniques) and gap-filled NEE and friction velocity, and estimated GPP (Level 4 products contain two GPP estimates; we used those derived from the method of Reichstein et al. (2005), where TER estimates derived from a nocturnal NEE versus temperature relationship, which includes nighttime temperature coefficients that are allowed to vary by season, are extrapolated to daytime and used to calculate GPP from NEE measurements, $GPP = NEE - TER$; hereafter these GPP estimates will be denoted GPP_{TER}). Vertical CO₂ mole fraction profile data were obtained from the AmeriFlux repository or directly from site investigators. CO₂ measurements at all sites were made with in situ infrared gas analyzers with associated uncertainty that differed among sites, but is estimated to be in the range of 0.2-1.0 $\mu\text{mol mol}^{-1}$. Measured and estimated data (NEE, GPP_{TER} , friction velocity, CO₂ mole fraction) are reported herein as the mean of 8 midday half-hourly measurements centered on local noon unless otherwise indicated; negative NEE and GPP indicate uptake by the ecosystem.

Table 1 Characteristics of AmeriFlux sites evaluated in this study

Site	Latitude Longitude Elevation	Vegetation type	Flux (above- canopy) measure- ment height [m]	Canopy height [m]	Within- canopy CO ₂ measure- ment height [m] ^a	Leaf area index [m ² m ⁻²]	Citation
Harvard Forest ^b	42.54°N 72.17°W 340 m	Mixed Forest	29.0	23.0	18.3	5.5	Urbanski et al. (2007)
Morgan Monroe	39.32°N 86.41°W 275 m	Deciduous Broad-leaf Forest	46.0	27.0	16.0	4.9	Schmid et al. (2000)
Willow Creek	45.81°N 90.08°W 515 m	Deciduous Broad-leaf Forest	29.6	24.2	21.3	5.4	Cook et al. (2004)
Niwot Ridge	40.03°N 105.55°W 3050 m	Evergreen Needle- leaf Forest	21.5	11.5	9.0	4.2	Monson et al. (2002)
Kendall Grassland	31.74°N 109.94°W 1530 m	C ₄ Grassland	6.4	0.5	0.5	1.0	Scott et al. (2010)
Rosemoun t Soybean	44.71°N 93.09°W 260 m	Soybean Cropland	2.0	0.9	1.1	7.5	Griffis et al. (2005)

^aHeight at which the CO₂ difference from the above-canopy CO₂ measurement was calculated; the above-canopy CO₂ measurement height was at or near the flux measurement height for all sites except Morgan Monroe, where the above-canopy CO₂ measurement height was 32.0 m. Note that the within-canopy CO₂ measurement height is not actually within the canopy at the Rosemount Soybean site; there were no within-canopy CO₂ measurements at this site, thus 1.1 m was selected.

^bOnly site where OCS measurements were made, at 29.0 m and 2.0 m (within-canopy).

Harvard Forest: OCS Mole Fraction Measurements

Air samples were collected on the flux tower above (29.0 m) and within (2.0 m) the forest canopy within 2 hours of each other in paired electropolished stainless steel flasks (2.5-3.0 l). Flask air samples were analyzed, within approximately 2 weeks of sample collection, for OCS mole fraction with the National Oceanic and Atmospheric Administration's coupled gas chromatograph (GC)-mass spectrometer (MS) system as described in Montzka et al. (2004). Median replicate injection precision for OCS mole fraction measurement at ambient levels during 2000-2006 was 0.4 % (approximately 3000 samples), and 95 % of the time it was less than 1.3 % (Montzka et al. 2007). For each above- or within-canopy air sample collected, paired flasks were filled over 5-10 minutes, typically within three hours of local noon. Above-canopy samples were collected approximately once every two weeks throughout the year in 2005 and 2006, providing a total of 70 above-canopy OCS mole fraction measurements. In 2005, 10 sets of above- and within-canopy samples were collected approximately once per week during the spring; sample collection began on day of year (DOY) 111 (April 21), before bud break, and ended on DOY 166 (June 15), after leaf expansion was complete. In 2006, 14 sets of above- and within-canopy samples were collected approximately once per week during the growing season; sample collection began on DOY 160 (June 9), after leaf expansion was complete, and ended on DOY 296 (October 23), near the time leaves fell. In 2006, two more sets of above- and within-canopy samples were collected after the growing season. In previous studies (Montzka et al. 2004; 2007), OCS measurements were discarded when paired samples disagreed by more than 1.3 % (approximately $6.3 \text{ pmol mol}^{-1}$). Only 9 of the 96 total OCS mole fraction measurements from the paired flask samples collected were outside of this rejection threshold, with the highest paired sample difference being $12.5 \text{ pmol mol}^{-1}$ (2.6 %) and only one other being greater

than $8.1 \text{ pmol mol}^{-1}$ (1.7 %). We retained these nine measurements in order to maximize the amount of data for analysis.

Harvard Forest: CO₂ Mole Fraction and CO₂ Flux Measurements

CO₂ mole fractions at eight heights (ranging from 0.3 m to 29.0 m) in the forest were determined by sequentially sampling each height through a series of solenoid valves mounted on the flux tower. Sample pressure was held constant (66.7 kPa) by modulating the flow to a bypass pump using a pressure controller (MKS, model 250B). A sub-sample was drawn through a Nafion dryer and -20 °C cold trap into a CO₂ analyzer (LI-COR, model 6251), configured for differential measurement using a reference gas at near ambient CO₂ (approximately $380 \text{ } \mu\text{mol mol}^{-1}$). Pressure in the analyzer cell was maintained constant (64.0 kPa) using a second pressure controller. The CO₂ analyzer was calibrated approximately every 4 hours with two working standards that spanned the typical range of ambient mole fractions. The working standards were calibrated to within $0.1 \text{ } \mu\text{mol mol}^{-1}$ or better in the laboratory before and after use against a set of World Meteorological Organization primary standards (NOAA-GMD; <http://www.esrl.noaa.gov/gmd/cc/ll/index.html>). Ambient mole fractions were computed from a linear fit through the two calibration standards.

CO₂ fluxes were determined by eddy covariance using a second CO₂ analyzer (LI-COR, model 6262), configured for fast response. The instrumental gain for the fast-response analyzer was determined by standard addition calibration using a small volume of 1 % CO₂ in air mixed into the sample flow (Goulden et al. 1996) and cross-checked by regressing the fast-response analyzer signal against the observed profile mole fraction for the time intervals when the two analyzers were sampling from the same height.

Harvard Forest: CO₂ and OCS Gradients and Ecosystem Relative Uptake (ERU)

CO₂ gradients were calculated by taking the difference between CO₂ mole fractions at 18.3 m (top of canopy is approximately 23.0 m) and 29.0 m (flux measurement height) and dividing by the measurement height difference. The 18.3 m measurement height was used for CO₂ gradient calculation because CO₂ drawdown was maximal at this within-canopy height; at lower heights CO₂ mole fractions were highly influenced by soil respiration (Fig. 2a). Ideally, CO₂ and OCS mole fraction gradients should be calculated with measurements from co-located sampling heights, but OCS mole fractions were only measured at 2.0 m and 29.0 m. OCS gradients were calculated with two methods. First, a linear OCS gradient between 29.0 m and 2.0 m was assumed and gradients were calculated by taking the difference between OCS mole fractions at 2.0 m and 29.0 m and dividing by the measurement height difference. Second, it was assumed that the shape of OCS profile was similar to the concurrently measured ozone (O₃) profile (Figs. 2b and 2c); OCS mole fractions were approximated for 18.3 m (co-located with the within-canopy CO₂ mole fraction measurement) were from this measured O₃ gradient. Plant canopies are an O₃ sink through leaf O₃ uptake, surface O₃ deposition, and O₃ reactions with plant-produced volatile organic compounds (VOCs) within the canopy air space. Some studies have shown that O₃ reaction with VOCs dominate over leaf O₃ uptake through stomata (Goldstein et al. 2004; Kurpius and Goldstein 2003), whereas others have found a larger dominance of stomatal O₃ uptake (Munger et al. 1996; Turnipseed et al. 2009). Thus, the O₃ profile is not an excellent OCS profile analog. However, leaf O₃ uptake, surface O₃ deposition, and O₃ reactions with VOCs are all within-canopy processes, as is leaf OCS uptake through stomata. Given that OCS data were available at only two heights, 2.0 m and 29.0 m, both methods to derive OCS gradients were used in subsequent calculations and results were compared. OCS profiles and gradients will be referred to as either linear or O₃-shaped.

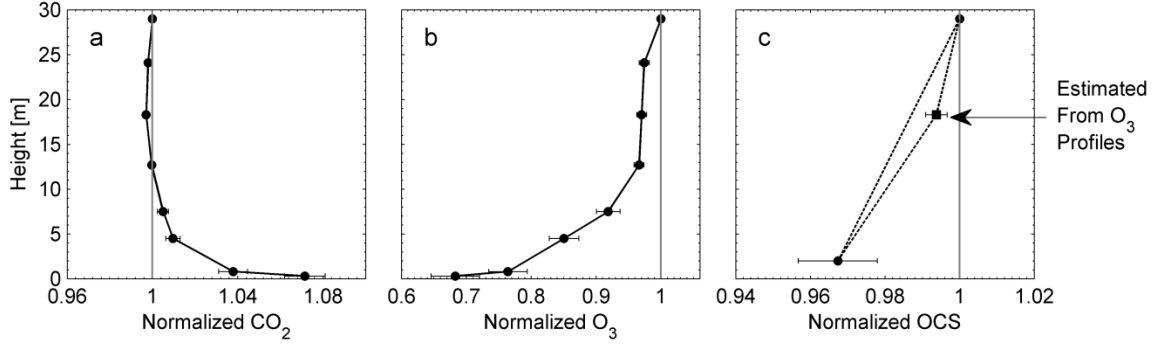


Fig. 2 Measured within-canopy gas profiles at Harvard Forest. Mean normalized **a** CO₂, **b** O₃, and **c** OCS mole fraction profiles calculated from the 12 days during the 2006 growing season when OCS measurements were made. Normalized mole fractions were calculated by dividing the mole fraction at each height by the mole fraction at 29.0 m; error bars show standard deviation of the mean at each height (in some cases error bars are smaller than symbols). Two OCS profiles are shown: linear profile between 29.0 and 2.0 m (the only two heights at which OCS mole fractions were measured) and an OCS profile with an estimated datum at 18.3 m (square symbol in **c**), which was based on the shape of the O₃ profiles measured at the time of air sample collection for OCS analysis and calculated from Eq. 7. OCS data were typically collected within 3 hours of local noon and within- and above-canopy measurements were typically made within less than 2 hours of each other; CO₂ and O₃ data are mean values calculated from half-hourly means corresponding to the time of OCS measurements.

The OCS mole fraction at 18.3 m (OCS_{18m}) was estimated from measured OCS mole fractions at 29.0 m and 2.0 m (OCS_{29m} and OCS_{2m}, respectively) and O₃ mole fractions at 29.0 m, 18.3 m, and 2.0 m (O_{3-29m}, O_{3-18m}, and O_{3-2m}, respectively; O_{3-2m} was calculated by linearly interpolating the O₃ mole fraction measurements at 4.5 m and 0.8 m):

$$\text{OCS}_{18\text{m}} = \text{OCS}_{29\text{m}} - (\text{OCS}_{29\text{m}} - \text{OCS}_{2\text{m}}) \left(\frac{\text{O}_{3-29\text{m}} - \text{O}_{3-18\text{m}}}{\text{O}_{3-29\text{m}} - \text{O}_{3-2\text{m}}} \right) \quad (7)$$

where OCS mole fractions are [pmol mol⁻¹] and O₃ mole fractions are [nmol mol⁻¹]. O₃ mole fractions were measured at the same heights as CO₂ mole fractions by sequentially sampling through the same series of solenoid valves mounted on the flux tower (Horii et al. 2004; Munger et al. 1998). A sub-sample was drawn directly from the sample manifold into a UV-absorbance

O₃ analyzer (Dasibi 1008, model TEI49c). Calibration of the O₃ analyzer was checked periodically by supplying known O₃ mole fractions from a factory calibrated O₃ generator/analyzer.

Measured CO₂ gradients and OCS gradients (from the linear OCS profiles) were linearly regressed against NEE and GPP_{TER}, respectively, to evaluate the influence of vegetation uptake on gradients (OCS gradients were not used to directly estimate OCS uptake or GPP, only to partition measured NEE as described below). CO₂ gradients were analyzed relative to NEE because CO₂ is both assimilated and released by the forest. OCS gradients were analyzed relative to GPP_{TER} because OCS is presumably taken up by the forest, but not released. CO₂ and OCS gradients were also linearly regressed against friction velocity to evaluate the influence of turbulence and atmospheric mixing. CO₂ mole fraction, NEE, GPP_{TER}, and friction velocity were calculated by averaging mean half-hourly values over the time period of the within- and above-canopy OCS measurements (typically a 2 hour or shorter time period). In addition to analysis of OCS gradients calculated from OCS mole fraction measurements, anticipated OCS gradients were estimated from measured CO₂ gradients and regressed against GPP_{TER} and friction velocity. These anticipated OCS gradients, estimated from only CO₂ gradients, are hereafter referred to as projected OCS gradients and were calculated with Eqs. 2-4, assuming co-located measurement heights for OCS and CO₂, an ERU of 4, and an above-canopy OCS mole fraction of 400 pmol mol⁻¹ (these assumptions produce projected OCS gradients for the same time frame and height difference as the CO₂ gradients). Projected OCS gradients allow a comparison to the measured OCS gradients at Harvard Forest and to projected OCS gradients from the other AmeriFlux sites (described below).

Two calculations of ERU were made. First, ERU was calculated with Eqs. 2-4 from time periods when simultaneous within- and above-canopy OCS and CO₂ measurements were available; this yielded nine individual ERU values (1 from 2005 and 8 from 2006) representative

of midday conditions when the measurements were made; hereafter these ERU values will be referred to as short-term ERU. Short-term ERU could not be calculated on 5 days (1 day from 2005 and 4 days from 2006) because either the CO_2 or OCS gradient, or both, were positive, indicating strong vertical mixing or less uptake compared to other days. Second, ERU was calculated as the slope of the line between a plot of the 12 corresponding relative OCS gradients and relative CO_2 gradients from the 2006 growing season; this method yielded a single ERU value representative of the 2006 growing season and hereafter will be referred to growing season ERU. Though a total of 26 paired flask samplings (above- and within-canopy) were obtained during 2005 and 2006, in 2005 only two sets and in 2006 only 12 sets of above- and within-canopy samples were available for ERU calculation because corresponding CO_2 mole fraction measurements were only available for these subsets of the OCS data.

Harvard Forest: Comparison of GPP Estimates and Uncertainties

Estimates of GPP from OCS-based NEE partitioning, hereafter denoted GPP_{OCS} , were calculated from Eq. 5 using short-term and growing season ERU and NEE measurements from the flux tower. This requires a value for LRU in Eq. 5, which was estimated from Eq. 6 by assuming $C_{\text{iCO}_2} / C_{\text{aCO}_2} = 0.79$ (value given by Seibt et al. (2010) for cool deciduous forests) and $g_{\text{sOCS}} / g_{\text{iOCS}} = 0.20$ and $C_{\text{mOCS}} / C_{\text{aOCS}} = 0.08$ (approximate values given by Stimler et al. (2010a) for C_3 species), yielding $\text{LRU} = 3.0$, which is within the uncertainty of the global mean LRU estimate, 2.8 ± 0.3 , reported by Seibt et al. (2010). GPP_{OCS} estimates were then compared to GPP_{TER} estimates for the time periods coincident with ERU values. GPP_{TER} uncertainty was assumed to be 20 %, based on calculations that accounted for choice of partitioning algorithm and data gaps (Desai et al. 2008). GPP_{OCS} uncertainty was calculated by propagating the uncertainties of NEE, ERU, and LRU through the calculation of GPP_{OCS} from Eq. 5 using standard error propagation techniques (Taylor 1997). Uncertainty for the NEE measurements at Harvard Forest was

assumed to be $2.3 \mu\text{mol m}^{-2} \text{s}^{-1}$ (Richardson et al. 2006). Uncertainty for ERU was calculated from the CO_2 and OCS gradient measurements for short-term ERU (O_3 gradient measurements were included in the ERU uncertainty calculation from the O_3 -shaped OCS profiles), and was calculated as the standard error of the slope of the line between the plot of relative OCS gradients and relative CO_2 gradients for growing season ERU. Measurements of LRU were not made, but Seibt et al. (2010) and Stimler et al. (2010a) reported approximate ranges of 1.5 to 4.0 and 1.0 to 4.0, respectively. The approximated LRU of 3 for Harvard Forest lies within these ranges and an arbitrary uncertainty of 1.5 (approximately half the reported LRU ranges) was assigned because 3 ± 1.5 approximates these ranges.

Harvard Forest: Estimation of OCS Flux Magnitude and Above-canopy OCS Gradients

Fluxes of OCS for 2006 were estimated from Eq. 1 using GPP_{TER} , above-canopy CO_2 and OCS mole fraction measurements, and an LRU of 3 (again, calculated from Eq. 6 assuming $C_{\text{iCO}_2} / C_{\text{aCO}_2} = 0.79$, $g_{\text{sOCS}} / g_{\text{iOCS}} = 0.20$, and $C_{\text{mOCS}} / C_{\text{aOCS}} = 0.08$). This provided estimates of the GPP-driven OCS flux at Harvard Forest for comparison with previous studies where canopy-scale OCS flux was measured. Above-canopy OCS mole fraction gradients ($\partial\text{OCS} / \partial z$) were estimated from the OCS flux estimates via Monin-Obukhov Similarity Theory (MOST), assuming neutral conditions (Wyngaard 2010):

$$\frac{\partial\text{OCS}}{\partial z} = \frac{\text{OCS}_*}{kz} \quad (8)$$

where OCS_* is OCS flux divided by friction velocity, k is the von Kármán constant (assumed to be 0.4), and z is height above the surface (29.0 m; flux measurement height). In order to produce

OCS gradients in units of $[\text{pmol mol}^{-1} \text{ m}^{-1}]$, $\partial\text{OCS} / \partial z$ from Eq. 8 was divided by the molar density of air $[\text{mol m}^{-3}]$ calculated from measured air temperature. This provided estimates of the GPP-driven surface layer OCS gradients over the canopy at Harvard Forest, which are useful to estimate analytical requirements for future studies.

Projection of OCS Gradients at Additional AmeriFlux Sites

Calculation of projected OCS gradients at other flux tower sites allowed comparison to Harvard Forest and evaluation of the potential magnitude of OCS signals at sites where OCS measurements have not yet been made. Measured CO_2 gradients and projected OCS gradients were calculated as described for Harvard Forest at five other AmeriFlux sites (Table 1). To project OCS gradients at Kendall Grassland, a warm-season C_4 grassland, we assumed an ERU of 4, as with the C_3 ecosystems. However, little work on OCS uptake has been done on C_4 leaves and in C_4 ecosystems. The assumption that C_4 ecosystems are similar to C_3 ecosystems is based on results from Sandoval-Soto et al. (2005), who found similar relative uptake ratios for corn leaves and C_3 leaves reported in the literature. We note, however, that CA activity is much lower in C_4 plants (Gillon and Yakir 2000), and this may mean our assumed ERU at Kendall Grassland was inappropriate. As with Harvard Forest, measured CO_2 gradients and projected OCS gradients were linearly regressed against NEE and GPP_{TER} , respectively, and friction velocity, to evaluate the influence of vegetation uptake and atmospheric mixing on measured gradients for CO_2 and anticipated gradients for OCS.

RESULTS

Harvard Forest

GPP_{TER} and above-canopy CO₂ and OCS mole fractions followed similar seasonal patterns in 2005 and 2006 at Harvard Forest (Fig. 3). The highest photosynthetic uptake rates (most negative GPP_{TER}) were near -40 $\mu\text{mol m}^{-2} \text{s}^{-1}$ in early summer, approximately halfway through the year. Seasonal decreases in CO₂ and OCS mole fractions above the canopy in spring were coincident with photosynthetic uptake, but minimum CO₂ lagged behind maximum GPP_{TER} in 2006, and minimum OCS lagged behind minimum CO₂ and even further behind maximum GPP_{TER}.

CO₂ gradients were linearly correlated with NEE and showed a trend of more drawdown (more negative gradients) with increasing NEE (Fig. 4a) ($y = 0.0053x + 0.015$, $r^2 = 0.16$, slope $P < 0.001$, intercept n.s.). CO₂ gradients were also correlated with friction velocity and showed more drawdown at lower friction velocity (Fig. 4c) ($y = 0.11x - 0.12$, $r^2 = 0.04$, slope $P < 0.025$, intercept $P < 0.001$). OCS gradients were correlated with GPP_{TER} and showed a trend of more drawdown with increasing GPP_{TER} (Fig. 4b) ($y = 0.015x - 0.085$, $r^2 = 0.17$, slope $P < 0.05$, intercept n.s.), similar to the relationship between CO₂ gradients and NEE. The relationship between OCS gradients and friction velocity was not significant (Fig. 4d) ($y = 0.66x - 0.70$, $r^2 = 0.09$, slope n.s., intercept $P < 0.05$).

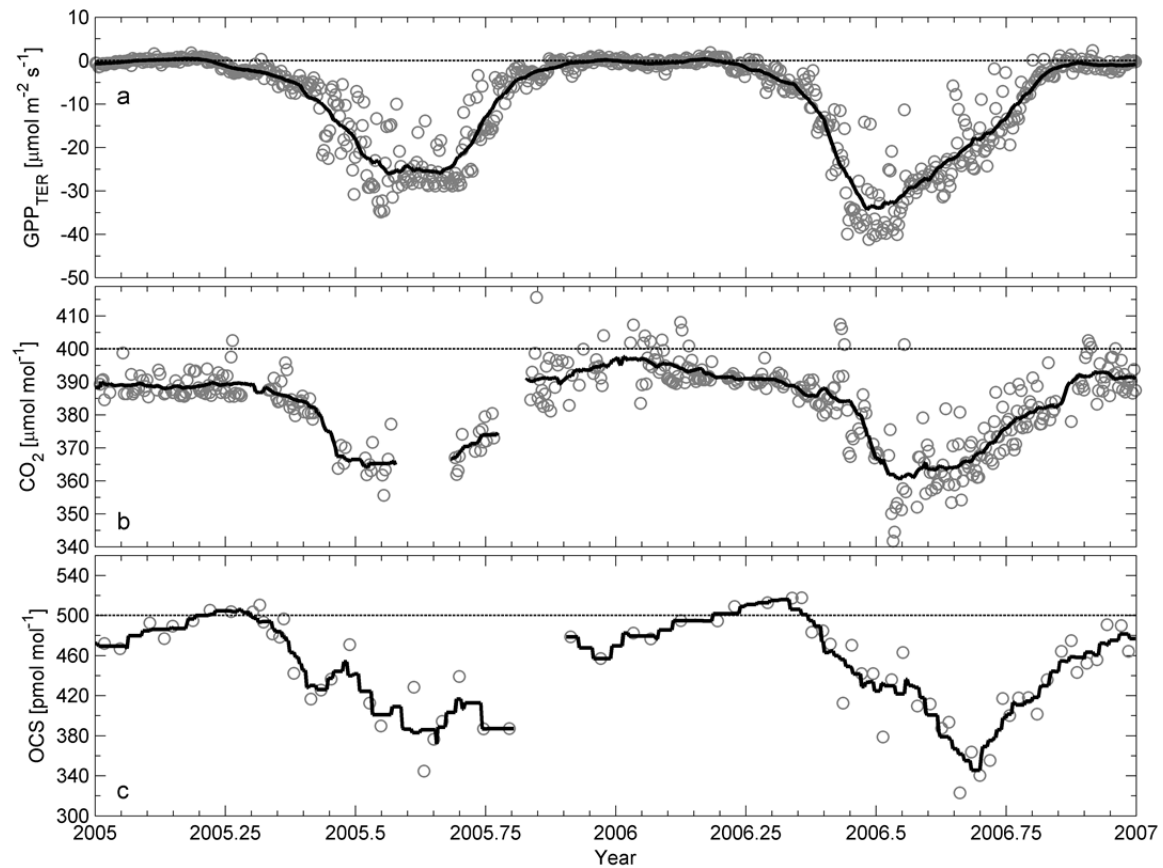


Fig. 3 Seasonal patterns of photosynthesis, and carbon dioxide (CO_2) and carbonyl sulfide (OCS) mole fractions at Harvard Forest. **a** Gross primary production estimates from net ecosystem exchange partitioning via the method of Reichstein et al. (2005) (GPP_{TER}), **b** CO_2 mole fraction measurements at 29.0 m, and **c** OCS mole fraction measurements at 29.0 m. GPP_{TER} and CO_2 data are mean values calculated from 8 half-hourly means centered on local noon; OCS data are from air samples typically collected within 3 hours of local noon. Solid lines are 31 day means centered on each day of year.

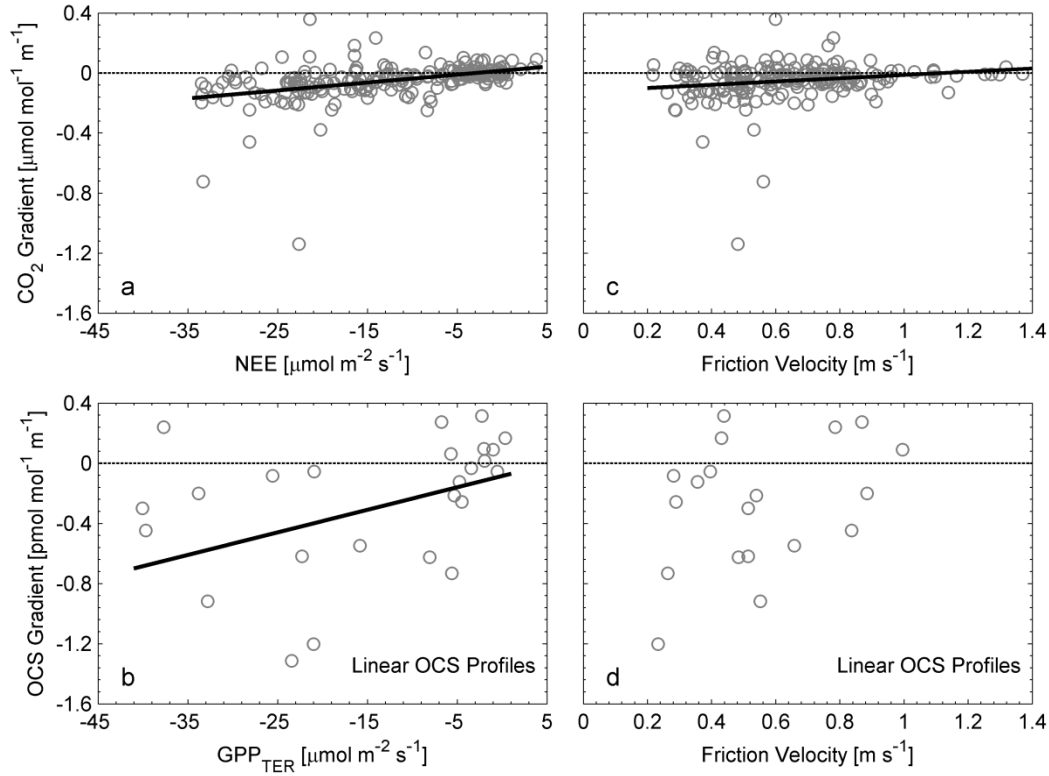


Fig. 4 Carbon dioxide (CO₂) and carbonyl sulfide (OCS) gradients as a function of driving variables Harvard Forest. CO₂ gradients (CO₂ at 18.3 m minus CO₂ at 29.0 m, divided by the height difference) versus **a** net ecosystem exchange (NEE) ($y = 0.0053x + 0.015$, $r^2 = 0.16$, slope $P < 0.001$, intercept n.s.) and **c** friction velocity ($y = 0.11x - 0.12$, $r^2 = 0.04$, slope $P < 0.025$, intercept $P < 0.001$). Harvard Forest OCS gradients, assuming a linear OCS profile (OCS at 2.0 m minus OCS at 29.0 m, divided by the height difference), versus **b** gross primary production estimates from NEE partitioning via the method of Reichstein et al. (2005) (GPP_{TER}) ($y = 0.015x - 0.085$, $r^2 = 0.17$, slope $P < 0.05$, intercept n.s.) and **d** friction velocity ($y = 0.66x - 0.70$, $r^2 = 0.09$, slope n.s., intercept $P < 0.05$). OCS data were typically collected within 3 hours of local noon and within-canopy and above-canopy measurements were typically made within less than 2 hours of each other; CO₂, NEE, GPP_{TER}, and friction velocity data points are mean values calculated from half-hourly means corresponding to the time of OCS measurements.

Relative OCS gradients were linearly correlated with relative CO₂ gradients, regardless of the method used to interpolate the available OCS data to derive gradients (Fig. 5; data are from the 2006 growing season only). Regressions were similar for linear OCS profiles (Fig. 5a; $y = 4.26x - 0.00$, $r^2 = 0.61$, slope $P < 0.01$, intercept n.s.) and O₃-shaped OCS profiles (Fig. 5b; $y = 3.28x + 0.00$; $r^2 = 0.76$; slope $P < 0.001$; intercept n.s.). The slopes of the lines (4.3 ± 0.6 in Fig. 5a and 3.3 ± 0.6 in Fig. 5b) represent growing season ERU values for 2006. Short-term ERU values

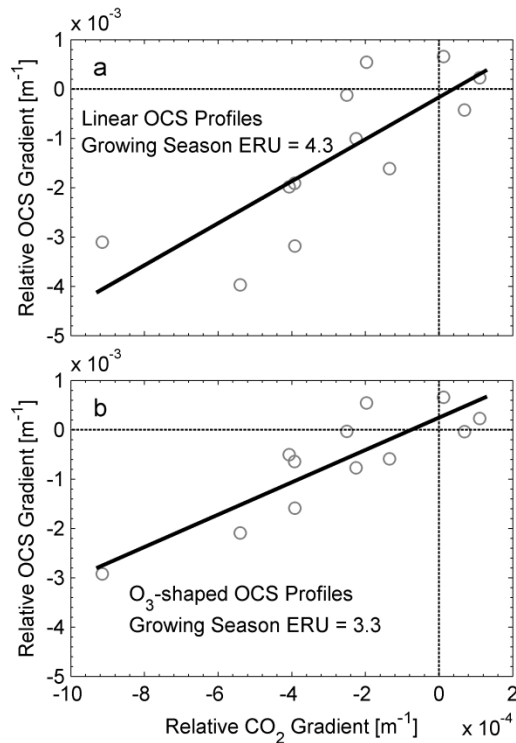


Fig. 5 Relative OCS gradients (calculated from Eq. 2) versus relative CO₂ gradients (calculated from Eq. 3) at Harvard Forest. CO₂ gradients were directly calculated from mole fraction measurements at 29.0 m and 18.3 m. OCS gradients were calculated for the 29.0 m and 18.3 m height difference using mole fraction measurements at 29.0 m and 2.0 m and **a** assuming a linear profile between 29.0 m and 2.0 m ($y = 4.26x - 0.00$, $r^2 = 0.61$, slope $P < 0.01$, intercept n.s.), and **b** estimating the OCS mole fraction at 18.3 m based on the shape of the O₃ profiles measured at the time of air sample collection for OCS analysis (Eq. 7) ($y = 3.28x + 0.00$; $r^2 = 0.76$; slope $P < 0.001$, intercept n.s.). Data are from the 2006 growing season only, and slopes of the lines are representative of ERU over the time period when the data were collected, day of year 160 to 296. OCS data were typically collected within 3 hours of local noon and within- and above-canopy measurements were typically made within less than 2 hours of each other; CO₂ data are mean values calculated from half-hourly means corresponding to the time period of OCS measurements.

(ratio of the relative OCS gradient to the relative CO₂ gradient for each datum) from 2006 ranged from 0.5 to 12.0 with a mean of 5.7 ± 1.2 (standard deviation of the mean) for ERU from linear OCS profiles and 0.1 to 4.4 with a mean of 2.8 ± 0.5 (standard deviation of the mean) for ERU from O₃-shaped OCS profiles. Data on DOY 166, 173, 272, and 296 were not included in the calculation of mean short-term ERU because CO₂ and/or OCS gradients were positive and near zero, indicating strong vertical mixing, near balance between uptake and release, or no uptake.

NEE and GPP_{TER} on DOY 166 and 173 were near $-30 \mu\text{mol m}^{-2} \text{s}^{-1}$ and comparable to other days during the middle of the growing season, however, friction velocity was also higher on these days (0.88 and 0.79 m s^{-1} , respectively) compared to other days during the middle of the growing season (friction velocity was typically less than 0.6 m s^{-1}). On DOY 272 and 296, near the end of the growing season, NEE and GPP_{TER} were low, less than $-7 \mu\text{mol m}^{-2} \text{s}^{-1}$, compared to other days during the middle growing season, and friction velocity was also high (0.87 and 1.00 m s^{-1} , respectively). Vertical mixing and/or near zero uptake may have contributed to the near zero and/or positive gradients on DOY 166, 173, 272, and 296.

Estimates of GPP_{OCS} calculated from NEE and short-term ERU (data from Fig. 5) in Eq. 5, assuming $LRU = 3$ (calculated from Eq. 6), were relatively consistent with the 1:1 line and correlated to GPP_{TER} (Figs. 6a and 6b) ($y = 1.26x - 4.31$; $r^2 = 0.77$, $P < 0.1$ (slope), s.e. of slope = 0.62 for ERU from linear OCS profiles; $y = 0.82x + 2.30$; $r^2 = 0.44$, $P < 0.05$ (slope), s.e. of slope = 0.35 for ERU from O_3 -shaped OCS profiles). Estimates of GPP_{OCS} calculated from NEE and growing season ERU (constant ERU = 4.3 from linear OCS profiles and ERU = 3.3 from O_3 -shaped OCS profiles) in Eq. 5 were similar in magnitude to GPP_{TER} (Fig. 6c) ($y = 1.28x + 3.11$, $r^2 = 0.99$, slope $P < 0.001$, s.e. of slope = 0.01 for ERU = 4.3 ; $y = 0.99x + 2.39$, $r^2 = 0.99$, slope $P < 0.001$, s.e. of slope = 0.01 for ERU = 3.3). It is important to note, however, when growing season ERU is used to estimate GPP_{OCS} (Fig. 6c), variability originates from variability in NEE, just as variability in GPP_{TER} originates from variability in NEE. Thus, the high correlation (Fig. 6c) is driven by NEE variability, as growing season ERU represents a constant scaling factor, along with LRU, used in Eq. 5 to partition NEE. On average, when using growing season ERU, GPP_{OCS} estimates were greater than GPP_{TER} by $3.6 \mu\text{mol m}^{-2} \text{s}^{-1}$ with a standard deviation of $3.2 \mu\text{mol m}^{-2} \text{s}^{-1}$ for ERU = 4.3 , and less than GPP_{TER} estimates by $2.7 \mu\text{mol m}^{-2} \text{s}^{-1}$ with a standard deviation of $0.9 \mu\text{mol m}^{-2} \text{s}^{-1}$ for ERU = 3.3 . When GPP was summed over DOY 160-296, for all daylight hours, GPP_{OCS}

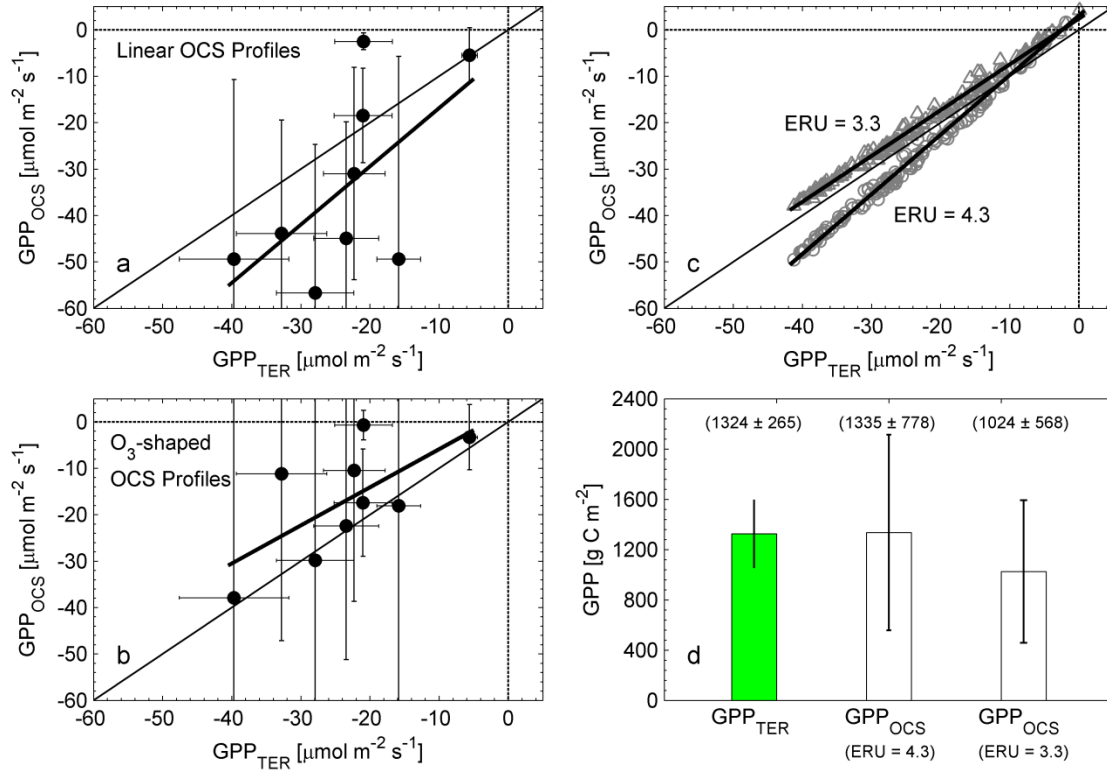


Fig. 6 Harvard Forest gross primary production estimates from net ecosystem exchange partitioning via the method of Reichstein et al. (2005) (GPP_{TER}) and Eq. 5 (GPP_{OCS}). In **a** and **b** GPP_{OCS} was calculated for 9 different days based on the short-term ERU estimate for each day; ERU was estimated from the **a** linear OCS profile ($y = 1.26x - 4.31$, $r^2 = 0.37$, $P < 0.1$), and **b** O_3 -shaped OCS profile ($y = 0.82x + 2.30$, $r^2 = 0.44$, $P < 0.05$). In **c** and **d** GPP_{OCS} was derived from NEE scaled by the growing season ERU values taken from the slopes of the lines in Fig. 5 (ERU from linear OCS profiles = 4.3 and ERU from O_3 -shaped OCS profiles = 3.3). OCS measurements spanned day of year 160 to 296 in 2006; **b** mean midday GPP for all days ($y = 1.28x + 3.11$, $r^2 = 0.99$, slope $P < 0.001$, s.e. of slope = 0.01 for $ERU = 4.3$ and $y = 0.99x + 2.39$, $r^2 = 0.99$, slope $P < 0.001$, s.e. of slope = 0.01 for $ERU = 3.3$) and **d** sum of GPP during daylight hours for all days. In all panels leaf relative uptake (LRU in Eq. 5) was estimated as 3 (calculated from Eq. 6). OCS data were typically collected within 3 hours of local noon and within- and above-canopy measurements were typically made within less than 2 hours of each other; GPP_{TER} data are mean values calculated from half-hourly means corresponding to the time period of OCS measurements.

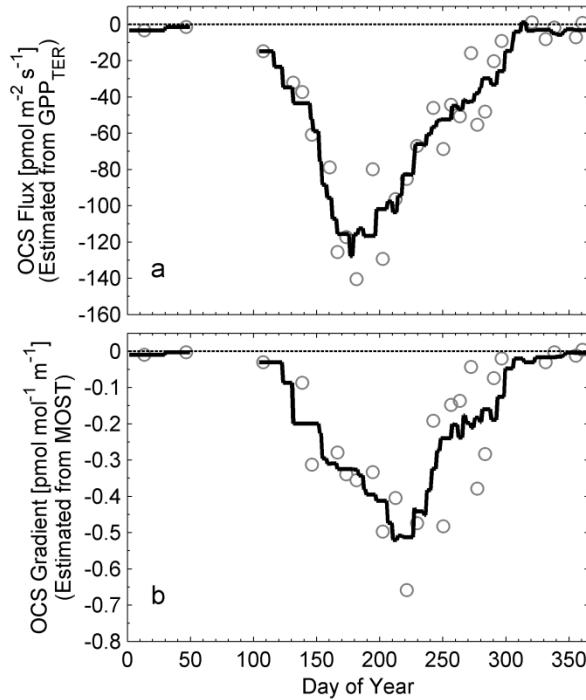


Fig. 7 Estimates of above-canopy carbonyl sulfide (OCS) fluxes and gradients at Harvard Forest. **a** OCS fluxes estimated from gross primary production estimates from net ecosystem exchange partitioning via the method of Reichstein et al. (2005) (GPP_{TER}) and **b** above-canopy (surface layer) OCS gradients estimated from Monin-Obukhov Similarity Theory (MOST) for 2006. OCS flux estimates were calculated from Eq. 1 using only above-canopy CO_2 and OCS mole fraction measurements and GPP_{TER} . Leaf relative uptake (LRU in Eq. 1) was estimated as 3 (calculated from Eq. 6). OCS gradient estimates were calculated from Eq. 8 using the OCS flux estimates from **a** and friction velocity measurements at 29.0 m (flux measurement height). GPP_{TER} and CO_2 data used to estimate OCS fluxes and friction velocity data used to estimate OCS gradients were mean values calculated from 8 half-hourly means centered on local noon; OCS data used in the estimate were from air samples typically collected within 3 hours of local noon. The solid line is a 31 day mean centered on each day of year. Only data from 2006 are shown because simultaneous above-canopy CO_2 and OCS measurements were unavailable due to missing CO_2 data on many of the days in 2005.

calculated with $ERU = 4.3$ was 1 % higher than GPP_{TER} , and GPP_{OCS} calculated with $ERU = 3.3$ was 23 % lower than GPP_{TER} (Fig. 6d).

Estimated OCS fluxes from Eq. 1, using GPP_{TER} estimates and assuming $LRU = 3$ (calculated from Eq. 6), ranged from approximately 0 to $-140 \text{ pmol m}^{-2} \text{ s}^{-1}$ (negative sign indicates assimilation) during 2006 (Fig. 7a), with a range of approximately -10 to $-140 \text{ pmol m}^{-2} \text{ s}^{-1}$ when leaves were present on trees. Estimated above-canopy (surface layer) OCS gradients

from Eq. 8, assuming OCS flux estimates were representative of GPP-driven flux, ranged from approximately 0 to $-0.6 \text{ pmol mol}^{-1} \text{ m}^{-1}$ (negative sign indicates drawdown) during 2006 (Fig. 7b).

Anticipated OCS Gradients at the Additional Sites

Measured CO_2 gradients and projected OCS gradients were linearly correlated with NEE and GPP_{TER} , respectively, at the five other AmeriFlux sites (Table 2; Fig. 8; measurements and projections at Harvard Forest are included for comparison). Measured CO_2 gradients and projected OCS gradients were also correlated with friction velocity at all sites (data not shown). Data from two broadleaf deciduous forests (Morgan Monroe State Forest and Willow Creek), with similar canopy structure and GPP_{TER} seasonality and magnitude as Harvard Forest, showed similar CO_2 gradients and as a result similar projected OCS gradients, compared to each other and Harvard Forest. Data from a subalpine conifer forest (Niwot Ridge) showed lower GPP_{TER} relative to the other forest sites, but similar CO_2 gradients and projected OCS gradients. Data from a warm-season C_4 grassland (Kendall Grassland) and a C_3 agricultural ecosystem (Rosemount Soybean) showed much larger CO_2 gradients for similar NEE relative to the forests, and therefore, much larger projected OCS gradients for similar GPP_{TER} relative to the forests.

Measured CO_2 gradients and projected OCS gradients were summarized for all sites for comparison (Table 3). Gradients for the deciduous forests (Harvard Forest, Morgan Monroe State Forest, and Willow Creek) and the subalpine conifer forest (Niwot Ridge) were similar. Gradients for the warm season C_4 grassland (Kendall Grassland) and soybean crop (Rosemount Soybean) were approximately 4 and 20 times greater than gradients at the forest site with the highest gradients (Willow Creek), respectively.

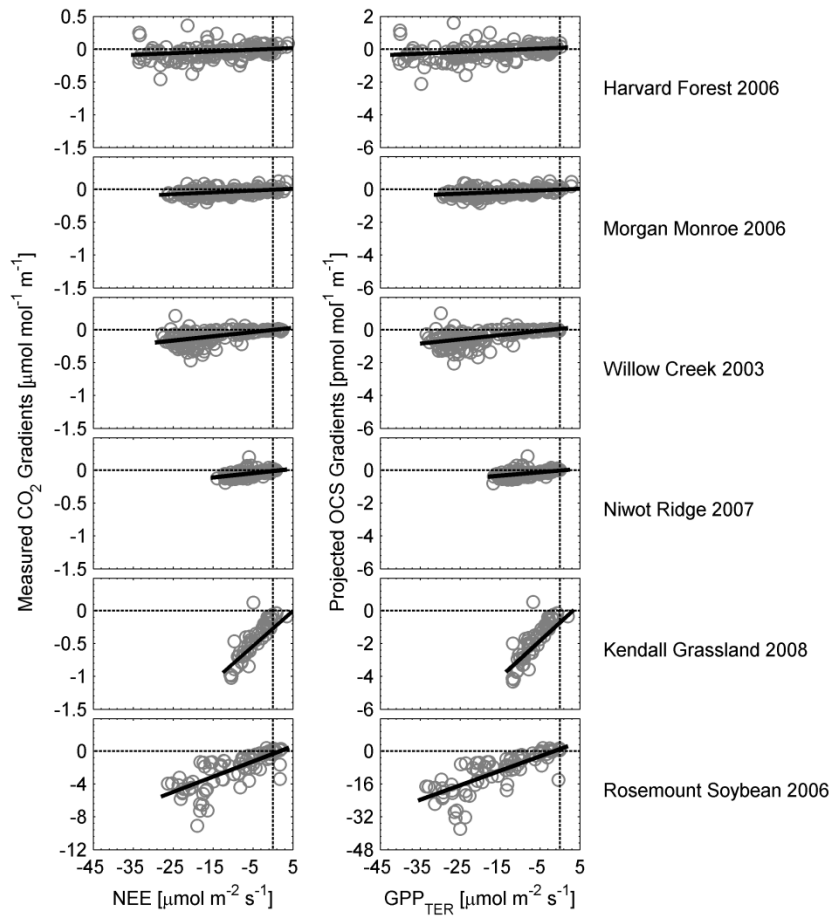


Fig. 8 Relationship between measured CO_2 gradients (within- minus above-canopy CO_2 mole fraction, divided by the difference between measurement heights) and measured net ecosystem exchange (NEE) (left panels), and projected OCS gradients and gross primary production estimates from NEE partitioning via the method of Reichstein et al. (2005) (GPP_{TER}) (right panels), at all six AmeriFlux sites evaluated. Projected OCS gradients were calculated with Eqs. 2-4, assuming co-located measurement heights for OCS and CO_2 , an ecosystem relative uptake (ERU) of 4, and an above-canopy OCS mole fraction of $400 \mu\text{mol mol}^{-1}$ (assumptions produce projected OCS gradients for the same time frame and height difference as CO_2 gradients). All data are mean values calculated from 8 half-hourly means centered on local noon. AmeriFlux site details are given in Table 1, statistics for the linear regressions are given in Table 2, and summary statistics for CO_2 and OCS gradients at each site are given in Table 3.

Table 2 Summary of linear regression statistics for measured CO₂ mole fraction gradients versus net ecosystem exchange (NEE) and projected OCS mole fraction gradients versus gross primary production (GPP_{TER}) at all sites evaluated (site details are provided in Table 1)

Site	Measured CO ₂ gradients ^a versus NEE			Projected OCS gradients ^b versus GPP		
	Slope ^c	Intercept ^d	r ²	Slope ^c	Intercept ^d	r ²
Harvard Forest	0.0034	0.0021	0.12	0.014	0.052	0.12
Morgan Monroe	0.0030	-0.0038	0.20	0.011	-0.0052	0.17
Willow Creek	0.0068	-0.0024	0.32	0.027	0.076	0.32
Niwot Ridge	0.0083	0.0045	0.41	0.026	0.030	0.36
Kendall Grassland	0.072	-0.11	0.78	0.30	0.041	0.75
Rosemount Soybean	0.20	-0.27	0.61	0.76	1.69	0.65

^aCalculated by taking the difference between within- and above-canopy CO₂ measurements, at the heights reported in Table 1, and dividing the CO₂ difference by the measurement height difference.

^bCalculated from measured CO₂ gradients via Eqs. 2-4, assuming co-located measurement heights for OCS and CO₂, ecosystem relative uptake (ERU) was 4, and above-canopy OCS mole fraction was 400 pmol mol⁻¹ (assumptions produce projected OCS gradients for the same time frame and height difference as CO₂ gradients).

^cAll slopes were significantly different from zero at the P < 0.001 level; units are μmol mol⁻¹ m⁻¹ / μmol m⁻² s⁻¹ and pmol mol⁻¹ m⁻¹ / μmol m⁻² s⁻¹ for CO₂ and OCS, respectively.

^dUnits are μmol mol⁻¹ m⁻¹ and pmol mol⁻¹ m⁻¹ for CO₂ and OCS, respectively.

Table 3 Summary of measured CO₂ mole fraction gradients and projected OCS mole fraction gradients at all sites evaluated (site details are provided in Table 1)

Site	Measured CO ₂ gradients ^a [μmol mol ⁻¹ m ⁻¹]				Projected OCS gradients ^b [pmol mol ⁻¹ m ⁻¹]			
	Mean	St. dev.	Min.	Max.	Mean	St. dev.	Min.	Max.
Harvard Forest	-0.04	0.10	-0.46	0.36	-0.18	0.44	-2.13	1.61
Morgan Monroe	-0.04	0.05	-0.19	0.12	-0.18	0.20	-0.83	0.51
Willow Creek	-0.10	0.11	-0.46	0.22	-0.43	0.47	-2.05	1.02
Niwot Ridge	-0.05	0.05	-0.19	0.20	-0.20	0.19	-0.79	0.85
Kendall Grassland	-0.45	0.28	-1.02	0.13	-1.90	1.18	-4.31	0.54
Rosemount Soybean	-2.04	2.14	-9.08	0.38	-8.89	9.37	-37.82	1.56

^aCalculated by taking the difference between within- and above-canopy CO₂ measurements, at the heights reported in Table 1, and dividing the CO₂ difference by the measurement height difference.

^bCalculated from measured CO₂ gradients via Eqs. 2-4, assuming co-located measurement heights for OCS and CO₂, ecosystem relative uptake (ERU) was 4, and above-canopy OCS mole fraction was 400 pmol mol⁻¹ (assumptions produce projected OCS gradients for the same time frame and height difference as CO₂ gradients).

DISCUSSION

Harvard Forest

The seasonal patterns of above-canopy CO₂ and OCS mole fractions at Harvard Forest in 2005 and 2006 were closely related (Fig. 3), as has been shown for previous years (Montzka et al. 2007). Seasonal dynamics of both gases were also related to the seasonal pattern of GPP_{TER} (Fig. 3). The peak-to-peak seasonal change in the above-canopy OCS mole fraction was approximately 150 pmol mol⁻¹, compared to a peak-to-peak seasonal change of approximately 30 μmol mol⁻¹ for the above-canopy CO₂ mole fraction. When the minimum summertime OCS mole fraction was referenced to a late winter/early spring OCS maximum of approximately 500 pmol mol⁻¹ and the minimum CO₂ mole fraction was referenced to a late winter/early spring CO₂ maximum of approximately 390 μmol mol⁻¹, the relative regional net uptake of OCS was approximately 4 times that of CO₂. This is slightly lower than the mean hemispheric value derived in Montzka et al. (2007), who reported that the relative variation in the OCS mole fraction seasonal amplitude at multiple sites in the northern hemisphere (including Harvard Forest, and coastal and marine sites that may be influenced by factors beyond uptake by vegetation) during 2000-2005 averaged 6 ± 1 times larger than the relative variation in the CO₂ mole fraction seasonal amplitude. The summer minimum in CO₂ mole fraction represents the point in time where CO₂ uptake and emission are equal over the broad region influencing mole fractions measured at Harvard Forest. After the minimum, emission is presumably greater than uptake and CO₂ mole fraction increases. For the OCS mole fraction, the summer minimum was considerably later (approximately 6-8 weeks) than that for CO₂ (Figs. 3b and 3c). This is likely

due in part to a lack of OCS release analogous to respiratory release of CO₂, thus the OCS mole fraction decreases until OCS uptake no longer occurs. Increase at the point of measurement occurs due to transport of background air with higher mole fraction.

At Harvard Forest, CO₂ gradients were correlated with NEE (Fig. 4a) and OCS gradients were correlated with GPP_{TER} (Fig. 4b), but strong relationships between gradients and fluxes are not necessarily expected because the magnitude of gradient for a given flux depends on intensity of vertical mixing. At higher friction velocity, mixing of within- and above-canopy air was enhanced and CO₂ and OCS gradients were diminished as expected, even when NEE and GPP_{TER} were high (Figs. 4c and 4d). Thus, vertical mixing may have contributed to the near zero and/or positive gradients observed on some days (DOY 166 and 173 for OCS gradients), indicating the challenge of measuring ERU over short time periods. Previous studies have found larger OCS gradients under more stable conditions when mixing was reduced (Mihalopoulos and Nguyen 2001; White et al. 2010).

Despite differing within-canopy measurement heights and measurement time frames for OCS mole fractions and CO₂ and OCS gradients, relative OCS and CO₂ gradients were linearly correlated during the 2006 growing season (Fig. 5), suggesting the likelihood of similar mechanisms controlling their magnitude and dynamics during the daytime. Measured gradients were due in part to photosynthetic uptake, indicated by the relationships between gradients and CO₂ fluxes (Figs. 4a and 4b). However, CO₂ gradients result from the balance between uptake and release, whereas OCS gradients are assumed to be affected by uptake only. Thus, relative uptake of OCS should be greater than that of CO₂. Our results were consistent with this perspective, as ERU for the 2006 growing season (days 160 to 296) was 4.3 ± 1.1 (Fig. 5a), assuming a linear OCS profile, and 3.3 ± 0.6 (Fig. 5b), assuming an O₃-shaped OCS profile. Both of these values are lower than the ERU of 5.7 ± 2.1 reported by Campbell et al. (2008) for multiple

sites in the eastern U.S. However, measured ERU was similar to the relative uptake of OCS over CO_2 , approximately 4, calculated from peak-to-peak seasonal differences in OCS and CO_2 measured at Harvard Forest during 2005-2006.

If CO_2 dynamics were controlled by NEE and OCS dynamics were controlled by GPP, at least in part, then a negative y-intercept would be expected for a regression between relative OCS and CO_2 gradients. In other words, when the CO_2 gradient is zero (within- and above-canopy CO_2 mole fractions are equal), within-canopy OCS should be lower than above-canopy OCS because the OCS gradient is only influenced by uptake (there is no significant within-canopy OCS source like there is for CO_2). The y-intercepts of the regressions were not significantly different from zero (Fig. 5). This may be due to the limited number of data points overall, and particularly, the limited number of data points near the beginning and end of the growing season when uptake and gradients were small.

As relative CO_2 uptake becomes small and approaches zero, uncertainty in short-term ERU increases because small changes and/or uncertainty in CO_2 have a large impact. This likely influenced gradient measurements on DOY 166, 173, 272, and 296, where ERU could not be calculated because some gradients were positive. The influence of turbulence also likely influenced the gradients, as strong mixing typically produces a more uniform profile and can lead to near-zero or positive gradients. Thus, the slope of the regression line between relative OCS and CO_2 gradient measurements should provide a better measure of ERU (Fig. 5). As a result, growing season ERU should provide a better estimate of GPP_{OCS} as opposed to short-term ERU (Fig. 6). However, use of growing season ERU assumes ERU is constant and masks intra-seasonal variability, which may arise from variable NEE / GPP or LRU (Eq. 5). This study was limited to a few pairs of corresponding CO_2 and OCS gradient measurements, but future studies could potentially benefit from more frequent OCS and CO_2 gradient measurements.

GPP_{OCS} was weakly correlated with GPP_{TER} when short-term ERU values were used to estimate GPP_{OCS} , and uncertainty was approximately 70 % of GPP_{OCS} (Figs. 6a and 6b). A large fraction of the uncertainty was due to uncertainty in CO_2 gradients, thereby influencing ERU uncertainty, as OCS and CO_2 measurements were not exactly coincident in time; uncertainty in LRU also added significantly to GPP_{OCS} uncertainty. When ERU and LRU uncertainty were halved, GPP_{OCS} uncertainty was reduced to approximately 35 %. With different measurement timescales and differing within-canopy CO_2 and OCS measurement heights, short-term ERU values may not be accurate because different air volumes may be measured, leading to differences in GPP_{OCS} and GPP_{TER} .

When growing season ERU (Fig. 5) was used to derive GPP_{OCS} from NEE measurements reasonable agreement between GPP_{OCS} and GPP_{TER} was found (Figs. 6c and 6d), potentially indicating that errors from extrapolating profiles average out over a season. Potential problems in relating short-term gradients (air samples collected over minutes) to mean fluxes (30-minute NEE or GPP) (Figs. 6a and 6b), such as influence from sweeps/injections of air and/or non-stationarity, are less likely to influence the nominal relationship over a growing season (Figs. 6c and 6d). Midday GPP_{OCS} estimates from growing season ERU were higher than GPP_{TER} estimates on average when ERU from the linear OCS profile was used to estimate GPP_{OCS} (Fig. 6c; slope of the regression line = 1.28; mean of GPP differences showed GPP_{OCS} was approximately 4 % higher than GPP_{TER}), and lower GPP_{TER} when ERU from the O_3 -shaped OCS profile was used to estimate GPP_{OCS} (Fig. 6c; slope of the regression line = 0.99; mean of GPP differences showed GPP_{OCS} was approximately 3 % lower than GPP_{TER}). Total GPP summed over DOY 160-296 showed GPP_{OCS} calculated with ERU = 4.3 matched GPP_{TER} and GPP_{OCS} calculated with ERU = 3.3 was 23 % less than GPP_{TER} , but the uncertainty of GPP_{OCS} was approximately 55 % of total GPP (Fig. 6d). Much of this uncertainty is due to uncertainty in LRU. When LRU uncertainty was

halved, from 1.5 to 0.75, GPP_{OCS} uncertainty was reduced to approximately 40 % of total GPP. When ERU uncertainty was halved with LRU uncertainty, GPP_{OCS} uncertainty was reduced to approximately 30 % of total GPP. When ERU and LRU uncertainty were reduced by two-thirds, GPP_{OCS} was approximately 20 %, the estimated uncertainty for GPP_{TER} . Previous studies have found that different NEE partitioning methods provide different estimates of GPP (Desai et al. 2008; Griffis et al. 2004; Lasslop et al. 2010; Stoy et al. 2006). Differences between GPP_{TER} and GPP_{OCS} estimates may be due to lack of understanding of all ecosystem processes that influence OCS exchange, violation of R1-R4 (such as soil OCS uptake), non-constant ERU and/or LRU, OCS measurement limitations, and/or inaccurate partitioning of NEE via the method of Reichstein et al. (2005). More work needs to be done with OCS in micrometeorological studies to determine if R1-R4 are indeed met and if exceptions exist. In future studies, ERU should be calculated from OCS and CO_2 gradient measurements at a co-located sampling position and over the exact same time period.

Ultimately, direct measurement of OCS fluxes via eddy covariance and subsequent estimation of GPP via Eq. (1) is the best way to use OCS uptake as a GPP proxy. High frequency OCS mole fraction measurements have been made with a quantum cascade laser (QCL) in the laboratory (Stimler et al. 2010b), and show promise, but have not yet been made in the field, thus it is uncertain whether the precision is adequate for eddy covariance. Stimler et al. (2010b) reported a 1 Hz measurement precision of 50 pmol mol^{-1} for the QCL; the largest measured OCS difference between the 2.0 m and 29.0 m heights in this study was $-44 \text{ pmol mol}^{-1}$ (linear gradient of $-1.6 \text{ pmol mol}^{-1} \text{ m}^{-1}$), with the smallest difference being near zero and a mean gradient during the 2006 growing season of approximately $-0.5 \text{ pmol mol}^{-1} \text{ m}^{-1}$. Estimated above-canopy (surface layer) OCS gradients were somewhat smaller, which is expected above the canopy, and averaged $-0.3 \text{ pmol mol}^{-1} \text{ m}^{-1}$ for the growing season (Fig. 7b). These data

provide an estimate of the instrument capabilities required to resolve above-canopy gradients in future studies. Given lack of detailed information on OCS within and above vegetation canopies, we cannot use these to confidently predict above-canopy variability in an OCS time series which would be useful to specify requirements for eddy covariance. It is possible that precision may need to improve for eddy covariance. Continuous, fast-response measurements are a major advantage provided by laser technology, which is developing rapidly. Instrumentation capable of measuring OCS fluxes via eddy covariance could be used to provide continuous GPP estimates from Eq. (1), completely independent of NEE measurements.

Estimates of OCS fluxes from GPP_{TER} provide indication of the expected magnitude of vegetation uptake at the flux tower scale, assuming OCS flux is driven by plant uptake, and are also useful for determining OCS measurement requirements. Maximum estimated ecosystem OCS fluxes at Harvard Forest (approximately $-140 \text{ pmol m}^{-2} \text{ s}^{-1}$) (Fig. 7a) were similar to maximum fluxes reported by Xu et al. (2002) (approximately $-140 \text{ pmol m}^{-2} \text{ s}^{-1}$) for a spruce forest in Germany. Mean fluxes were in the same range, $-70 \pm 36 \text{ pmol m}^{-2} \text{ s}^{-1}$ at Harvard Forest and $-93 \pm 12 \text{ pmol m}^{-2} \text{ s}^{-1}$ from Xu et al. (2002) for daytime. These OCS flux estimates are one to two orders of magnitude larger than soil uptake fluxes reported in previous studies, which range from approximately 0 to $-10 \text{ pmol m}^{-2} \text{ s}^{-1}$ (Kesselmeier et al. 1999; Kuhn et al. 1999; Liu et al. 2010; Simmons et al. 1999; Steinbacher et al. 2004; White et al. 2010; Xu et al. 2002). If soil fluxes at Harvard Forest were similar to those from previous studies, then OCS flux estimates provide indication that plant uptake was the dominant flux. If other OCS fluxes, such as soil uptake or emission by vegetation (Berresheim and Vulcan 1992), are not negligible compared to vegetation uptake, then ERU measurements or ecosystem-scale flux measurements will contain contributions from these fluxes and will be different than expected if only plants were contributing to uptake, posing problems for using OCS as a GPP proxy.

Anticipated OCS Gradients at the Additional Sites

Measured CO₂ gradients at the other AmeriFlux sites were correlated to NEE (Table 2; Fig. 8), and projected OCS gradients were correlated to GPP_{TER} (Table 2; Fig. 8). This was expected because OCS gradients were directly projected from CO₂ gradients via an assumed ERU and above-canopy OCS mole fraction, and because GPP_{TER} is closely related to NEE via the NEE partitioning method (Reichstein et al. 2005). Nonetheless, projected OCS gradients are useful because within-canopy OCS measurements were only made at Harvard Forest in this study, thus projected gradients provide an indication of expected gradients and for determining OCS measurement requirements. Measured and projected OCS gradients plotted versus GPP_{TER} at Harvard Forest showed the slope from measured linear gradients, 0.015 (Fig. 4b), was very near the slope from projected gradients, 0.014 (Table 2; Fig. 8b). This is likely due to the assumed ERU of 4.0, which is near the measured growing season ERU of 4.3 calculated from linear OCS gradients. This provides some confidence that projected OCS gradients at other sites may be a reasonable estimate of actual OCS gradients at those sites, and thus required OCS measurement precision. Estimation of GPP_{OCS} from Eq. 5 requires accurate measurement of OCS and CO₂ gradients for ERU calculation in Eq. 4, indicating that the difference measurements required for gradient calculation are more important than absolute accuracy of mole fraction measurements. Thus measurement precision is more important than absolute accuracy using the ERU approach for estimating GPP_{OCS}.

At the other forest sites, projected OCS gradients were similar to the measured gradients, estimated surface layer gradients, and projected gradients at Harvard Forest (Table 3; Figs. 7b and 8). Maximum projected OCS gradients (largest negative values) at forest sites were comparable to current uncertainty in OCS measurement capabilities, approximately 0.5 % (S. Montzka unpublished data), which yields 1.5-2.8 pmol mol⁻¹ for OCS mole fractions ranging from

300-550 pmol mol⁻¹. However, other issues may affect the ability to discern small differences from flask samples, namely the potential of artifacts associated with sample storage and contamination. Despite challenges with flask sample measurements, results at Harvard Forest indicate ERU can be measured (Fig. 5), suggesting ERU is potentially measurable at other forest sites, particularly with the potential of high frequency, in-situ measurements that can be averaged over longer time periods (Stimler et al. 2010b). It is possible that OCS gradients at Harvard Forest were measurable because within-canopy OCS was measured near the soil surface at 2.0 m. If the entire canopy acted as an OCS sink, as has been suggested by previous studies where OCS profiles were measured (Mihalopoulos et al. 1989; Mihalopoulos and Nguyen 2001; White et al. 2010), the lowest OCS mole fractions would likely occur near the soil surface. It may be that OCS gradients would be difficult to measure at the same within-canopy height as CO₂ gradients due to OCS measurement limitations, but the previous studies where OCS profiles were measured provide some optimism. It should be noted that measured CO₂ gradients, and as a result the corresponding projected OCS gradients, were positive some of the time for all sites (Table 3; Fig. 8), indicating that within-canopy CO₂ uptake was sometimes outweighed by respiratory release, affected by mixing, and/or influenced by urban pollution. Positive values of projected OCS gradients calculated from measured CO₂ gradients are strictly a result of calculation from Eqs. 2-4. It is not anticipated that positive OCS gradients will always correspond to positive CO₂ gradients when actual OCS measurements are used for gradient calculation.

Projected OCS gradients in short canopies (C₄ grassland and soybean crop) were much greater than projected gradients in taller forest canopies for a given GPP (Table 3; Fig. 8), with maximum values greater than current uncertainty in OCS measurement capabilities. In light of the encouraging results from Harvard Forest reported herein, OCS measurements and resulting GPP_{OCS} estimates may be even more useful in short canopies. One of the main differences

between grassland or cropped agricultural ecosystems and forests is canopy height and structure, where photosynthesizing leaf area is contained within a small volume in grassland and agricultural ecosystems compared to forests. Even if forest canopies and shorter canopies have similar leaf area, it is spread over a much larger volume in forests, thus gradients are likely to be much smaller in forests than in short canopies, assuming similar NEE and GPP rates (Fig. 8). Additionally, mixing is often enhanced in forests relative to short canopies due to the aerodynamic roughness and relative openness of forest canopies. These distinctions are illustrated by comparing measured CO_2 and projected OCS gradients at Kendall Grassland and Niwot Ridge, which had similar NEE and GPP_{TER} rates (approximately -10 to $-15 \mu\text{mol m}^{-2} \text{s}^{-1}$, respectively) during the growing season. CO_2 gradients and OCS gradients were much larger in the grassland relative to the forest. On average, measured CO_2 gradients at Kendall grassland were approximately nine times greater than the measured CO_2 gradients at Niwot Ridge (Table 3), even with a lower leaf area index at Kendall Grassland (Table 1), resulting in projected OCS gradients at Kendall Grassland that were approximately 9 times greater than those at Niwot Ridge.

CONCLUSIONS

Prior studies have indicated the possibility of using OCS uptake as a GPP proxy. Clearly, GPP estimation via NEE partitioning from OCS measurements (Eq. 5) requires reduced uncertainty in ERU and LRU. Despite shortcomings in the OCS measurements (within-canopy CO₂ and OCS measurements were not co-located, within- and above-canopy OCS mole fraction measurements and CO₂ and OCS mole fraction measurements were not exactly coincident in time), estimates of GPP scaled from NEE measurements using measured ERU and estimated LRU produced results similar to a standard and widely applied NEE partitioning method for GPP estimation (Reichstein et al. 2005). This demonstrates potential utility of OCS in constraining GPP in micrometeorological studies, particularly as higher frequency and higher resolution OCS measurement instrumentation becomes available.

Given the need for accurate partitioning of NEE measurements into component fluxes, further studies of OCS uptake as a GPP proxy are warranted. More work is required to determine whether conditions R1-R4 are met at flux tower sites and whether exceptions exist at different sites. Specifically, characterization of plant OCS uptake relative to other ecosystem fluxes, namely soil exchange and the possibility of plant emission, is required. Leaf-level studies provide strong indication that the requirements R1-R4 are met, but most leaf-level studies have been performed under controlled conditions. An important next step towards using OCS uptake as a GPP proxy at the flux tower-scale is to further study OCS dynamics and exchange in various ecosystems. Specifically, better characterization of LRU variability is required, in addition to concurrent, co-located OCS and CO₂ above-canopy profile measurements and/or direct OCS flux

measurements, which allow GPP estimation and comparison to GPP estimates from currently applied NEE partitioning techniques. Investigations in short-statured canopies are likely to provide the most information in the near-term, while analytical instruments continue to improve.

REFERENCES

- Baldocchi DD, Wilson KB (2001) Modeling CO₂ and water vapor exchange of a temperate broadleaved forest across hourly to decadal time scales. *Ecol Model* 142:155-184
- Baldocchi D, Falge E, Gu L, Olson R, Hollinger D, Running S, Anthoni P, Bernhofer C, Davis K, Evans R, Fuentes J, Goldstein A, Katul G, Law B, Lee X, Malhi Y, Meyers T, Munger W, Oechel W, Paw U KT, Pilegaard K, Schmid HP, Valentini R, Verma S, Vesala T, Wilson K, Wofsy S (2003) FLUXNET: A new tool to study the temporal and spatial variability of ecosystem-scale carbon dioxide, water vapor, and energy flux densities. *Bull Amer Meteorol Soc* 82:2415-2434
- Bartell U, Hofmann U, Hofmann R, Kreuzburg B, Andreae MO, Kesselmeier J (1993) COS and H₂S fluxes over a wet meadow in relation to photosynthetic activity: An analysis of measurements made on 6 September 1990. *Atmos Environ* 27A:1851-1864
- Berresheim H, Vulcan VD (1992) Vertical distributions of COS, CS₂, DMS and other sulfur compounds in a loblolly pine forest. *Atmos Environ* 26A:2031-2036
- Blake NJ, Campbell JE, Vay SA, Fuelberg HE, Huey LG, Sachse G, Meinardi S, Beyersdorf A, Baker A, Barletta B, Midyett J, Doezema L, Kamboures M, McAdams J, Novak B, Rowland FS, Blake DR (2008) Carbonyl sulfide (OCS): Large-scale distributions over North America during INTEX-NA and relationship to CO₂. *J Geophys Res* 113:D09S90 doi:10.1029/2007JD009163
- Brown KA, Bell JNB (1986) Vegetation-The missing sink in the global cycle of carbonyl sulfide (COS). *Atmos Environ* 20:537-540
- Caird MA, Richards JH, Donovan LA (2007) Nighttime stomatal conductance and transpiration in C₃ and C₄ plants. *Plant Physiol* 143:4-10
- Campbell JE, Carmichael GR, Chai T, Mena-Carrasco M, Tang Y, Blake DR, Blake NJ, Vay SA, Collatz GJ, Baker I, Berry JA, Montzka SA, Sweeney C, Schnoor JL, Stanier CO (2008) Photosynthetic control of atmospheric carbonyl sulfide during the growing season. *Science* 322:1085-1088
- Castro MS, Galloway JN (1991) A comparison of sulfur-free and ambient air enclosure techniques for measuring the exchange of reduced sulfur gases between soils and the atmosphere. *J Geophys Res* 96:D8 427-437
- Cellier P, Brunet Y (1992) Flux-gradient relationships above tall plant canopies. *Agric For Meteorol* 58:93-117

- Cook BD, Davis KJ, Wang W, Desai A, Berger BW, Teclaw RM, Martin JG, Bolstad PV, Bakwin PS, Yi C, Heilman W (2004) Carbon exchange and venting anomalies in an upland deciduous forest in northern Wisconsin, USA. *Agric For Meteorol* 126:271-295
- Denmead OT, Bradley EF (1985) Flux-gradient relationships in a forest canopy. In: Hutchinson BA, Hicks BB (eds) *The Forest-Atmosphere Interaction*. Reidel, Norwell, Massachusetts, USA, pp 421-442
- Desai AR, Richardson AD, Moffat AM, Kattge J, Hollinger DY, Barr A, Falge E, Noormets A, Papale D, Reichstein M, Stauch VJ (2008) Cross-site evaluation of eddy covariance GPP and RE decomposition techniques. *Agric For Meteorol* 148:821-838
- Geng C, Mu Y (2004) Carbonyl sulfide and dimethyl sulfide exchange between lawn and the atmosphere. *J Geophys Res* 109:D12302 doi:10.1029/2003JD004492
- Gillon JS, Yakir D (2000) Naturally low carbonic anhydrase activity in C₄ and C₃ plants limits discrimination against C¹⁸OO during photosynthesis. *Plant Cell Environ* 23:903-915
- Goldan PD, Fall R, Kuster WC, Fehsenfeld FC (1988) Uptake of OCS by growing vegetation: A major tropospheric sink. *J Geophys Res* 93:14,186-14,192
- Goldstein AH, McKay M, Kurpius MR, Schade GW, Lee A, Holzinger R, Rasmussen RA (2004) Forest thinning experiment confirms ozone deposition to a forest canopy is dominated by reaction with biogenic VOCs. *Geophys Res Lett* 31:L22106 doi:10.1029/2004GL021259
- Goulden ML, Munger JW, Fan SM, Daube BC, Wofsy SC (1996) Measurements of carbon sequestration by long-term eddy covariance: methods and a critical evaluation of accuracy. *Glob Change Biol* 2:169-182
- Griffis TJ, Black TA, Gaumont-Guay D, Drewitt GB, Nesic Z, Barr AG, Morgenstern K, Kljun N (2004) Seasonal variation and partitioning of ecosystem respiration in a southern boreal aspen forest. *Agric For Meteorol* 125:207-223
- Griffis TJ, Baker JM, Zhang J (2005) Seasonal dynamics and partitioning of isotopic CO₂ exchange in a C₃/C₄ managed ecosystem. *Agric For Meteorol* 132:1-19
- Horii CV, Munger JW, Wofsy SC (2004) Fluxes of nitrogen oxides over a temperate deciduous forest. *J Geophys Res* 109:D08305 doi:10.1029/2003JD004326
- Kesselmeier J, Hubert A (2002) Exchange of reduced volatile sulfur compounds between leaf litter and the atmosphere. *Atmos Environ* 36:4679-4686
- Kesselmeier J, Merk L (1993) Exchange of carbonyl sulfide (COS) between agricultural plants and the atmosphere: Studies on the deposition of COS to peas, corn, and rapeseed. *Biogeochemistry* 23:47-59
- Kesselmeier J, Teusch N, Kuhn U (1999) Controlling variables for the uptake of atmospheric carbonyl sulfide by soil. *J Geophys Res* 104:11577-11584

- Kettle AJ, Kuhn U, von Hobe M, Kesselmeier J, Andreae MO (2002) Global budget of atmospheric carbonyl sulfide: Temporal and spatial variations of the dominant sources and sinks. *J Geophys Res* 107:D22 4658 doi:10.1029/2002JD002187
- Kluczewski SM, Brown KA, Bell JNB (1985) Deposition of [³⁵S]-carbonyl sulphide to vegetable crops. *Radiat Protect Dosim* 11:173-177
- Kuhn U, Ammann C, Wolf A, Meixner FX, Andreae MO, Kesselmeier J (1999) Carbonyl sulfide exchange on an ecosystem scale: soil represents a dominant sink for atmospheric COS. *Atmos Environ* 33:995-1008
- Kurpius MR, Goldstein AH (2003) Gas-phase chemistry dominates O₃ loss to a forest, implying a source of aerosols and hydroxyl radicals to the atmosphere. *Geophys Res Lett* 30:1371 doi:10.1029/2002GL016785
- Lasslop G, Reichstein M, Papale D, Richardson AD, Arneeth A, Barr A, Stoy P, Wohlfahrt G (2010), Separation of net ecosystem exchange into assimilation and respiration using a light response curve approach: critical issues and global evaluation. *Glob Change Biol* 16:187-208 doi:10.1111/j.1365-2486.2009.02041.x
- Lavigne MB, Ryan MG, Anderson DE, Baldocchi DD, Crill PM, Fitzjarrald DR, Goulden ML, Gower ST, Massheder JM, McCaughey JH, Rayment M, Striegl RG (1997) Comparing nocturnal eddy covariance measurements to estimates of ecosystem respiration made by scaling chamber measurements at six coniferous boreal sites. *J Geophys Res* 102:28,977-28,985
- Law BE, Ryan MG, Anthoni PM (1999) Seasonal and annual respiration of a ponderosa pine ecosystem. *Glob Change Biol* 5:169-182
- Liu J, Geng C, Mu Y, Zhang Y, Xu Z, Wu H (2010) Exchange of carbonyl sulfide (COS) between the atmosphere and various soils in China. *Biogeosciences* 7:753-762
- Mihalopoulos N, Bonsang B, Nguyen BC, Kanakidou M, Belviso S (1989) Field observations of carbonyl sulfide deficit near the ground: Possible implication of vegetation. *Atmos Environ* 23:2,159-2,166
- Mihalopoulos N, Nguyen BC (2001) Vertical distribution of carbonyl sulfide in a eucalyptus forest. *Chemos – Glob Change Sci* 3:275-282
- Monson RK, Turnipseed AA, Sparks JP, Harley PC, Scott-Denton LE, Sparks K, Huxman TE (2002) Carbon sequestration in a high-elevation, subalpine forest. *Glob Change Biol* 8:459-478
- Montzka SA, Tans PP (2004) Can carbonyl sulfide help constrain gross vegetative fluxes of carbon dioxide? *EOS Trans AGU* 85:Fall Meeting Supplement Abstract B21E-04
- Montzka SA, Aydin M, Battle M, Butler JH, Saltzman ES, Hall BD, Clarke AD, Mondeel D, Elkins JW (2004) A 350-year atmospheric history for carbonyl sulfide inferred from Antarctic firn air and air trapped in ice. *J Geophys Res* 109:D22302 doi:10.1029/2004JD004686

- Montzka SA, Calvert P, Hall BD, Elkins JW, Conway TJ, Tans PP, Sweeney C (2007) On the global distribution, seasonality, and budget of atmospheric carbonyl sulfide (COS) and some similarities to CO₂. *J Geophys Res* 112:D09302 doi:10.1029/2006JD007665
- Munger JW, Wofsy SC, Bakwin PS, Fan SM, Goulden ML, Daube BC, Goldstein AH, Moore KE, Fitzjarrald DR (1996) Atmospheric deposition of reactive nitrous oxides and ozone in a temperate deciduous forest and a subarctic woodland 1. Measurements and mechanisms. *J Geophys Res* 101:12,639-12,657
- Munger JW, Fan SM, Bakwin PS, Goulden ML, Goldstein AH, Colman AS, Wofsy SC (1998) Regional budgets for nitrogen oxides from continental sources: Variations of rates for oxidation and deposition with season and distance from source region. *J Geophys Res* 103:8355-8368
- Notni J, Schenk S, Protoschill-Krebs G, Kesselmeier J, Anders E (2007) The missing link in COS metabolism: Study on the reactivation of carbonic anhydrase from its hydrosulfide analogue. *ChemBioChem* 8:530-536
- Ogeé J, Brunet Y, Loustau D, Berbigier P, Delzon S (2003a) *MuSICA*, a CO₂, water and energy multilayer, multileaf pine forest model: evaluation from hourly to yearly time scales and sensitivity analysis. *Glob Change Biol* 6:697-1017.
- Ogeé J, Peylin P, Ciais P, Bariac T, Brunet Y, Berbigier P, Roche C, Richard P, Bardoux G, Bonnefond JM (2003b) Partitioning net ecosystem carbon exchange into net assimilation and respiration using ¹³CO₂ measurements: A cost-effective sampling strategy. *Glob Biogeochem Cycl* 17:1070 doi:10.1029/2002GB001995
- Ogeé J, Peylin P, Cuntz M, Bariac T, Brunet Y, Berbigier P, Richard P, Ciais P (2004) Partitioning net ecosystem carbon exchange into net assimilation and respiration with canopy-scale isotopic measurements: An error propagation analysis with ¹³CO₂ and CO¹⁸O data. *Glob Biogeochem Cycl* 18:GB2019 doi:10.1029/2003GB002166.
- Protoschill-Krebs G, Kesselmeier J (1992) Enzymatic pathways for the metabolism of carbonyl sulphide (COS) by higher plants. *Botanic Acta* 108:445-448
- Protoschill-Krebs G, Wilhelm C, Kesselmeier J (1996) Consumption of carbonyl sulphide (COS) by higher plant carbonic anhydrase (CA). *Atmos Environ* 30:3,151-3,156
- Puxbaum H, König G (1997) Observation of dipropenyldisulfide and other organic sulfur compounds in the atmosphere of a beech forest with *Allium ursinum* ground cover. *Atmos Environ* 31:291-294
- Raupach MR (1979) Anomalies in flux-gradient relationships over forest. *Bound Layer Meteorol* 16:467-486
- Reichstein M, Falge E, Baldocchi D, Papale D, Aubinet M, Berbigier P, Bernhoffer C, Buchmann N, Gilmanov T, Granier A, Grünwald T, Havránková K, Ilvesniemi H, Janous D, Knohl A, Laurila T, Lohila A, Loustau D, Matteucci G, Meyers T, Miglietta F, Ourcival J, Pumpanen J, Rambal S,

- Rotenberg E, Sanz M, Tenhunen J, Seufert G, Vaccari F, Vesala T, Yakir D, Valentini R (2005) On the separation of net ecosystem exchange into assimilation and ecosystem respiration: review and improved algorithm. *Glob Change Biol* 11:1-16 doi:10.1111/j.1365-2486.2005.001002.x
- Richardson AD, Hollinger DY, Burba GG, Davis KJ, Flanagan LB, Katul GG, Munger JW, Ricciuto DM, Stoy PC, Suyker AE, Verma SB, Wofsy SC (2006) A multi-site analysis of random error in tower-based measurements of carbon and energy fluxes. *Agric For Meteorol* 136:1-18 doi:10.1016/j.agrformet.2006.01.007
- Sacks WJ, Schimel DS, Monson RK, (2007) Coupling between carbon cycling and climate in a high-elevation, subalpine forest: a model-data fusion analysis. *Oecologia* 151:54-68 doi:10.1007/s00442-006-0565-2
- Sandoval-Soto L, Stanimirov M, von Hobe M, Schmitt V, Valdes J, Wild A, Kesselmeier J (2005) Global uptake of carbonyl sulfide (COS) by terrestrial vegetation: Estimates corrected by deposition velocities normalized to the uptake of carbon dioxide (CO₂). *Biogeosciences* 2:125-132
- Scanlon TM, Kustas WP (2010) Partitioning water vapor and carbon dioxide fluxes using correlation analysis. *Agric For Meteorol* 150:89-99
- Schmid HP, Grimmond CSB, Cropley F, Offerle B, Su HB (2000) Measurements of CO₂ and energy fluxes over a mixed hardwood forest in the mid-western United States. *Agric For Meteorol* 103:357-374
- Scott RL, Hamerlynck EP, Jenerette GD, Moran MS, Barron-Gafford G (2010) Carbon dioxide exchange in a semidesert grassland through drought-induced vegetation change. *J Geophys Res* 115:G03026 doi:10.1029/2010JG001348
- Seibt U, Kesselmeier J, Sandoval-Soto L, Kuhn U, Berry JA (2010) A kinetic analysis of leaf uptake of COS and its relation to transpiration, photosynthesis, and carbon isotope fractionation. *Biogeosciences* 7:333-341
- Simmons JS, Klemetsson L, Hultberg H, Hines ME (1999) Consumption of atmospheric carbonyl sulfide by coniferous boreal forest soils. *J Geophys Res* 104:11,569-11,576
- Steinbacher M, Bingemer HG, Schmidt U (2004) Measurements of the exchange of carbonyl sulfide (OCS) and carbon disulfide (CS₂) between soil and atmosphere in a spruce forest in central Germany. *Atmos Environ* 38:6043-6052
- Stimler K, Montzka SA, Berry JA, Rudich Y, Yakir D (2010a) Relationships between carbonyl sulfide (COS) and CO₂ during leaf gas exchange. *New Phytol* 186:869-878
- Stimler K, Nelson D, Yakir D (2010b) High precision measurements of atmospheric concentrations and plant exchange rates of carbonyl sulfide using mid-IR quantum cascade laser. *Glob Change Biol* 16:2496-2503 doi: 10.1111/j.1365-2486.2009.02088.x

- Stoy PC, Katul GG, Sequeira MBS, Juang JY, Novick KA, Uebelherr JM, Oren R (2006) An evaluation of models for partitioning eddy covariance-measured net ecosystem exchange into photosynthesis and respiration. *Agric For Meteorol* 141:2-18
- Suntharalingham P, Kettle AJ, Montzka SM, Jacob DJ (2008) Global 3-D model analysis of seasonal cycle of atmospheric carbonyl sulfide: Implications for terrestrial vegetation uptake. *Geophys Res Lett* 35:L19801 doi:10.1029/2008GL034332
- Taylor JR (1997) *An Introduction to Error Analysis*. University Science Books, Sausalito, California, USA.
- Turnipseed AA, Burns SP, Moore DJP, Hu J, Guenther AB, Monson RK (2009) Controls over ozone deposition to a high elevation subalpine forest. *Agric For Meteorol* 149:1447-1459
- Urbanski S, Barford C, Wofsy S, Kucharik C, Pyle E, Budney J, McKain K, Fitzjarrald D, Czikowsky M, Munger JW (2007) Factors controlling CO₂ exchange on timescales from hourly to decadal at Harvard Forest. *J Geophys Res* 112:G02020, doi:10.1029/2006JG000293
- Van Diest H, Kesselmeier J (2008) Soil atmosphere exchange of carbonyl sulfide (COS) regulated by diffusivity depending on water-filled pore space. *Biogeosciences* 5:475-483
- van Gorsel E, Delapierre N, Leuning R, Black A, Munger JW, Wofsy S, Aubinet M, Feigenwinter C, Beringer J, Bonal D, Chen B, Chen J, Clement R, Davis KJ, Desai AR, Dragoni D, Etzold S, Grünwald T, Gu L, Heinesch B, Hutrya LR, Jans WWP, Kutsch W, Law BE, Leclerc MY, Mammarella I, Montagnani L, Noormets A, Rebmann C, Wharton S (2009) Estimating nocturnal ecosystem respiration from the vertical turbulent flux and change in storage of CO₂. *Agric For Meteorol* 149:1919-1930
- Watt SF (2000) The mass budgets of carbonyl sulfide, dimethyl sulfide, carbon disulfide and hydrogen sulfide. *Atmos Environ* 34:761-779
- White ML, Zhou Y, Russo RS, Mao H, Talbot R, Varner RK, Sive BC (2010) Carbonyl sulfide exchange in a temperate loblolly pine forest grown under ambient and elevated CO₂. *Atmos Chem Phys* 10:547-561
- Wingate L, Ogeé J, Cuntz M, Genty B, Reiter I, Seibt U, Yakir D, Maseyk K, Pendall EG, Barbour MM, Mortazavi B, Burlett R, Peylin P, Miller J, Mencuccini M, Shim JH, Hunt J, Grace J (2009) The impact of soil microorganisms on the global budget of $\delta^{18}\text{O}$ in atmospheric CO₂. *Proc Nat Acad Sci* 106:22,411-22,415
- Wyngaard JC (2010) *Turbulence in the Atmosphere*. Cambridge University Press, New York, New York, USA.
- Xu X, Bingemer HG, Schmidt U (2002) The flux of carbonyl sulfide and carbon disulfide between the atmosphere and a spruce forest. *Atmos Chem Phys* 2:171-181
- Yi C, Li R, Bakwin PS, Desai A, Ricciuto DM, Burns SP, Turnipseed AA, Wofsy SC, Munger JW, Wilson K, Monson RK (2004) A nonparametric method for separating photosynthesis and

respiration components in CO₂ flux measurements. *Geophys Res Lett* 31:L17107
doi:10.1029/2004GL020490

Yonemura S, Sandoval-Soto L, Kesselmeier J, Kuhn U, von Hobe M, Yakir D, Kawahima S (2005)
Uptake of carbonyl sulfide (COS) and emissions of dimethyl sulfide (DMS) by plants. *Phyton*
45:17-24

Zha T, Xing Z, Wang KY, Kellomäki S, Barr AG (2007) Total and component carbon fluxes of a
Scots Pine ecosystem from chamber measurements and eddy covariance. *Ann Botany*
99:345-353

Zobitz JM, Burns SP, Reichstein M, Bowling DR (2008) Partitioning net ecosystem carbon
exchange and the carbon isotopic disequilibrium in a subalpine forest. *Glob Change Biol*
14:1785-1800 doi:10.1111/j.1365-2486.2008.01609.x